O-mode and X-mode coupling effects in toroidal plasmas at fundamental and second EC harmonics and implication for ITER

Vdovin V.L.

RRC Kurchatov Institute, Tokamaks Physics Institute

16th Joint Workshop on
Electron Cyclotron Emission and Electron Cyclotron Resonance Heating
12-15 April 2010
Haynan, Sanya China

OUTLINE

- **Recent updates of STELEC stellarator 3D full wave ECRH code**
  - **- account to non diagonal wave-plasma response terms**
  - **- mode conversion to EB waves**
  - **- boundary conditions**
  - **- Upper Hybrid Resonance $\omega^2 = \omega_{ce}^2 + \omega_{pe}^2$ importance**
    - **- broadness of cold ECR- UHR pair: $\Delta R \sim R\, n_e$**
  - **- Current strap antenna with/without Faraday Screen and plain/elliptical polarization**
- **Fundamental harmonic O-mode scenario in toroidal plasmas**
  - **- Precise validation of O- and X-mode coupling and broadened power deposition control by UHR position**

Second harmonic X-mode scenarios in tokamaks and ITER
  - **- X and O-mode coupling effects in under dense plasmas**
  - **- deposition peculiarities in spherical tokamaks**
- **O-X-B scenarios are included**

- **Conclusions**

ECRF out of diagonal wave induced Electron currents – important at quasi perpendicular launch

(stressed by Fidone et al & Litvak et al in geometrical optic treatment 1976)

$$J^{(1,1)} = \frac{c^2}{8\pi\omega}\{(\vec{e}_b\cdot\nabla)[(\hat{\zeta}_{-1}+\hat{\zeta}_{+1})\nabla_\perp\times E_b'\vec{e}_b - i(\hat{\zeta}_{-1}-\hat{\zeta}_{+1})(\nabla_\perp\times E_b'\vec{e}_b)\times\vec{e}_b]$$

$$+\vec{e}_b\left[\vec{e}_b\cdot\nabla_\perp\times\left[(\hat{\zeta}_{-1}+\hat{\zeta}_{+1})(\vec{e}_b\cdot\nabla)\vec{E}_\perp' - i(\hat{\zeta}_{-1}-\hat{\zeta}_{+1})(\vec{e}_b\cdot\nabla)(\vec{E}_\perp'\times\vec{e}_b)\right]\right]\}$$

$$\hat{\zeta}_{+1} = \frac{1}{4}\frac{\omega_{pe}^2}{\omega\omega_{ce}}\frac{v_{Te}^2}{c^2}\left\{-\mu^2F_{7/2}'(0) - 2\mu^2F_{7/2}'(1)\right\}$$

$$\hat{\zeta}_{-1} = \frac{1}{4}\frac{\omega_{pe}^2}{\omega\omega_{ce}}\frac{v_{Te}^2}{c^2}\left\{-\mu^2F_{7/2}'(0) - 2\left(\frac{\omega}{\omega+\omega_{ce}}\right)^2\right\}$$

ECH out of plasma fundamental resonance O-mode launch high resolution modelling at low frequency strongly validate that EBWs play crucial role in toroidal plasmas

- Motivation

WEGA stellarator fundamental harmonic O-mode ECH experiments at 6 GHz, Podoba Yu. Radio frequency heating on the WEGA stellarator, *PHD thesis, Ernst-Moritz-Arndt-Universität Greifswald. 2006*

Out of plasma cold electron fundamental cyclotron resonance at HFS
- efficient ECRF heating with two groups heated electrons: fast electrons group and warm electrons

Our idea to explain the result was that main Heating role play Electron Bernstein Waves born at Upper Hybrid Resonance and well trapped in core plasma

O-X-B modes coupling at EC out off plasma fundamental harmonic in DIII-D/WEGA-like oblique $N_{//}=0.32$ O-mode outside launch, F=6 GHz, Bo=0.16 T, $N_e(0)=2.3\ 10^{17}\ m^{-3}$, $T_e(0)=9.2$ kV,

at $N_e < N_{crit}|_{O\text{-mode}}$, EBW –red colour

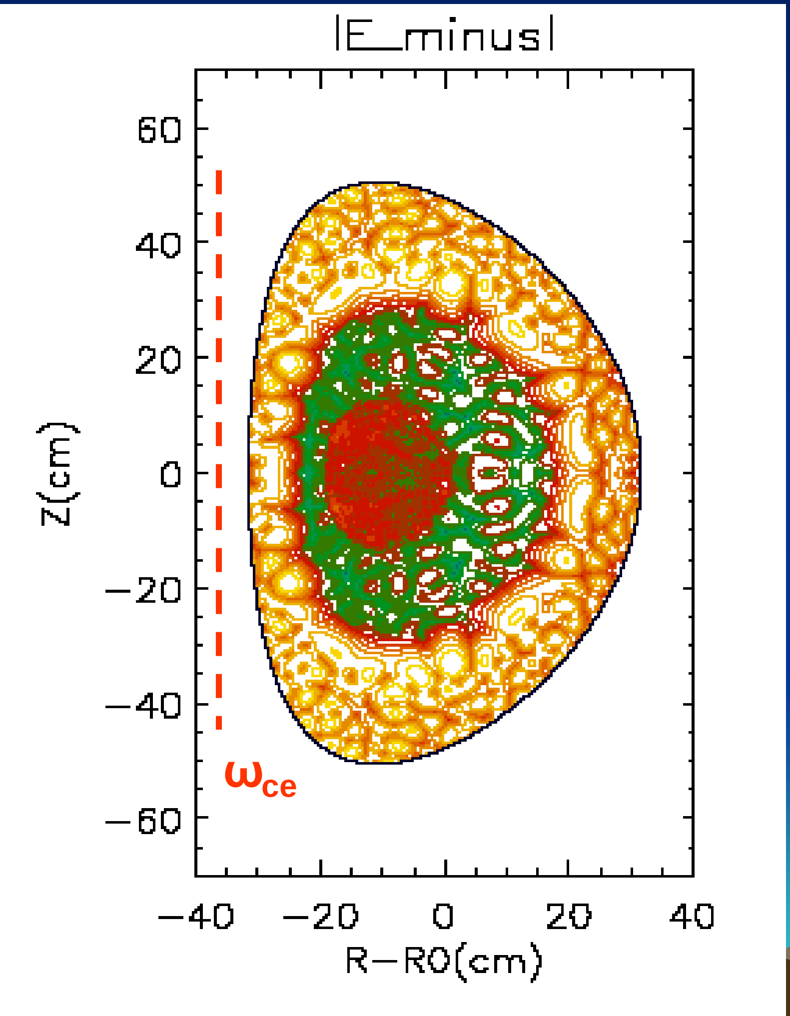

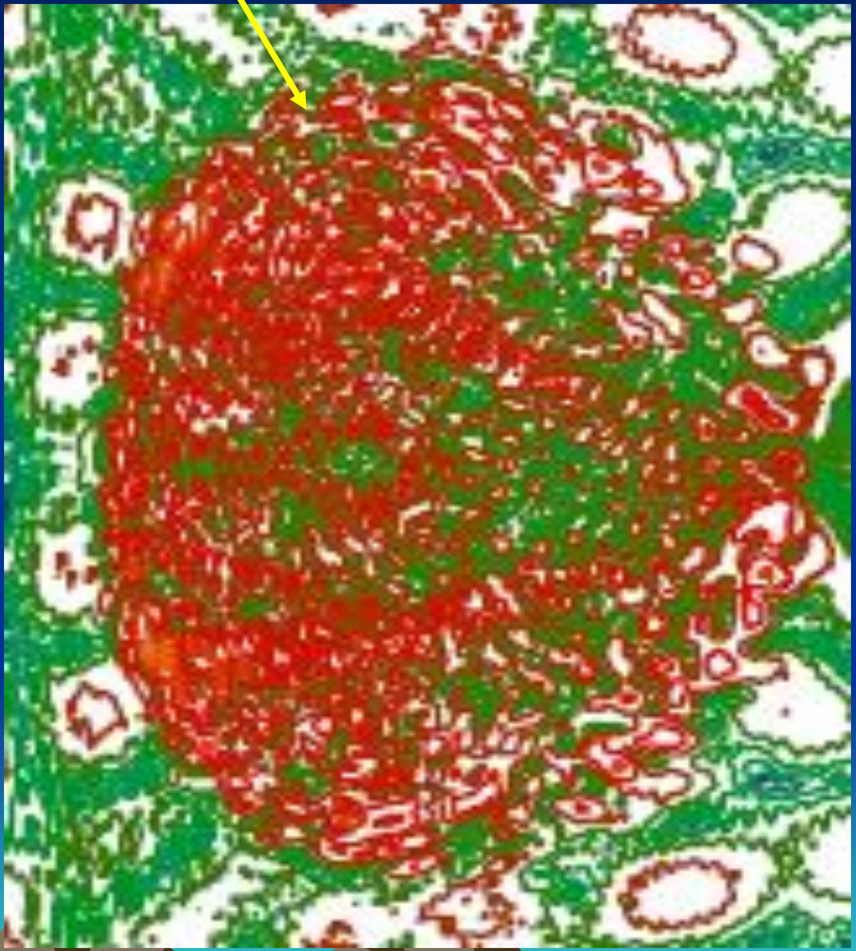

Radial power deposition profile in DIII-D/WEGA-like at oblique O-mode launch, $N_{//}$=0.3 $Pe(2\omega_{ce})$ = 61% (red), $Pe(\omega_{ce})$ = 39%

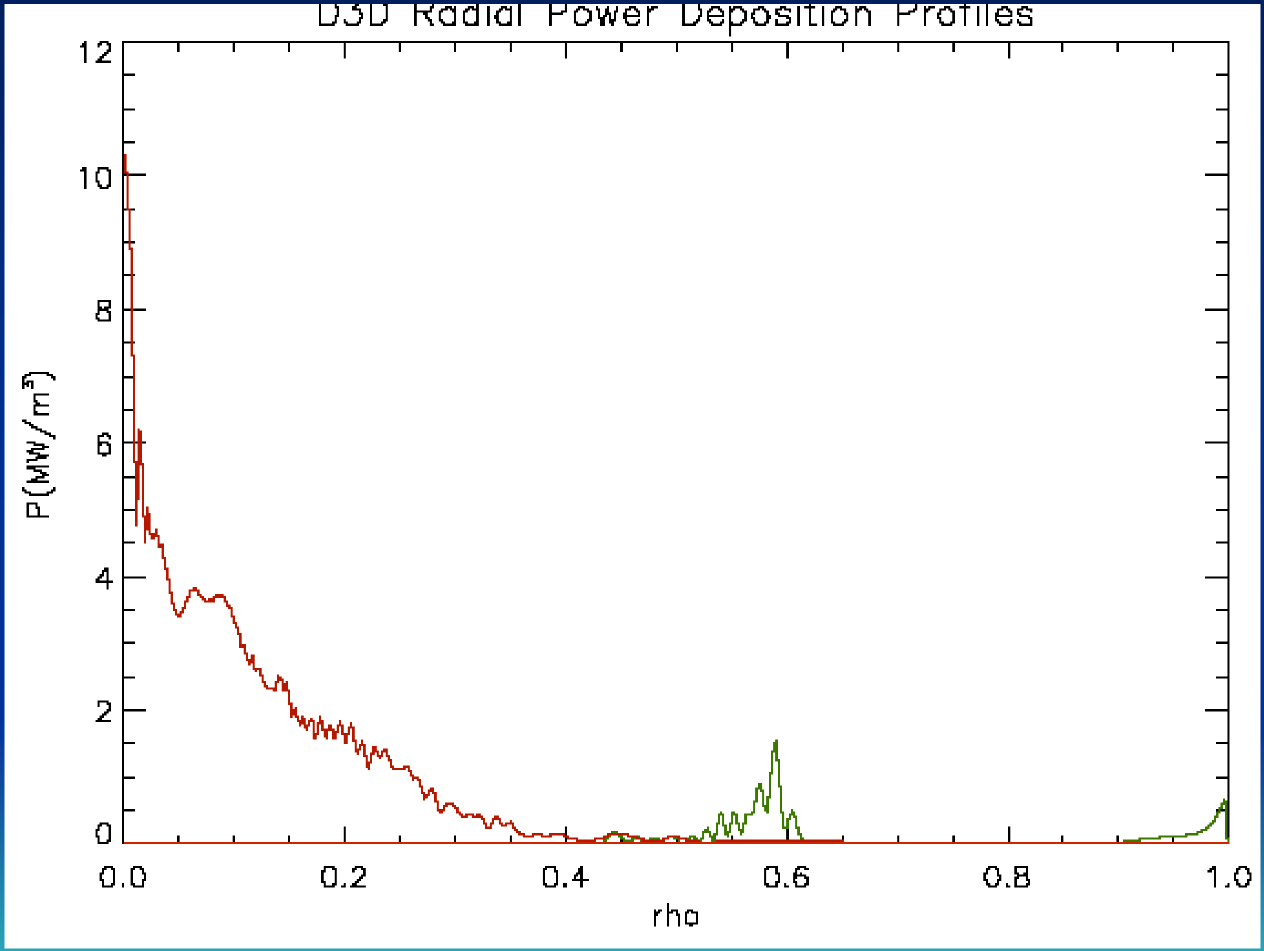

O-X-B modes coupling at EC out off plasma fundamental harmonic in T-10-like O-mode quasi perpendicular $N_{//}$=0.016 outside launch at $N_e < N_{crit}|_{O\text{-mode}}$ |E_minus|

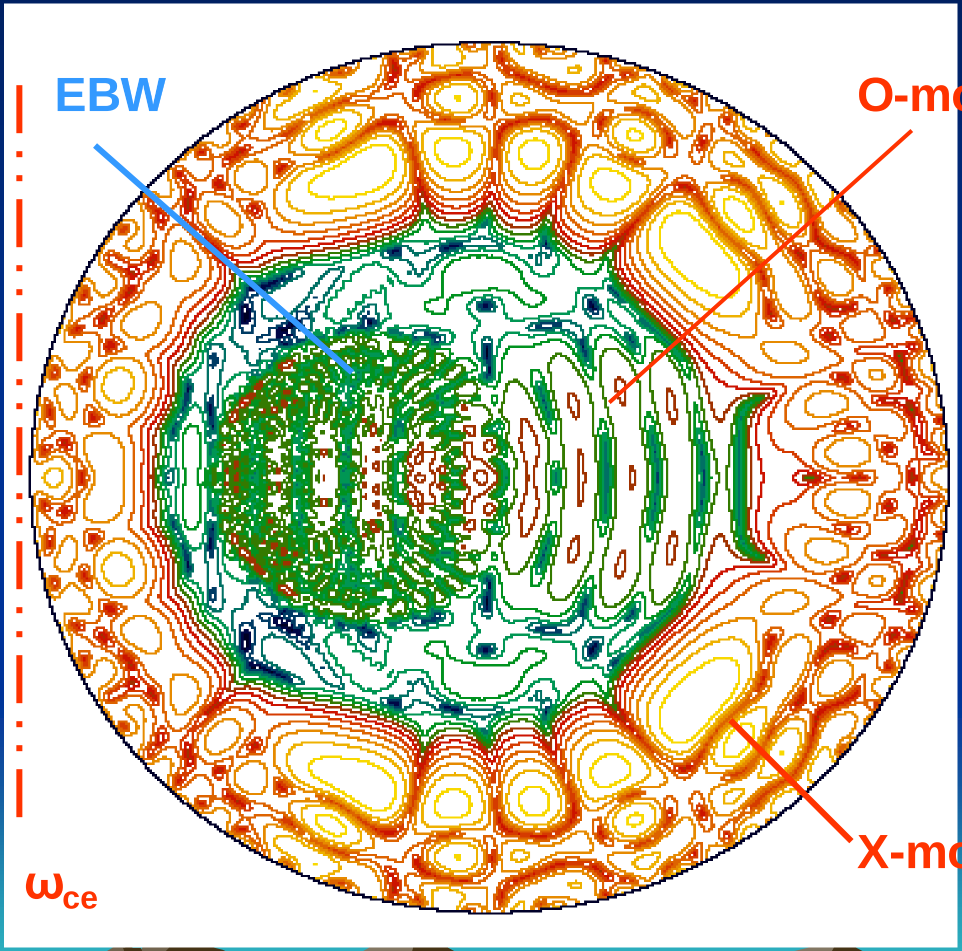

Radial power deposition profile in T-10/WEGA like at ECR out off plasma perpendicular O-mode launch, $N_{//}=0.016$ at $N_e < N_{crit}|_{O\text{-mode}}$, $P_e(2\omega) = 100\%$ -by EBW absorption

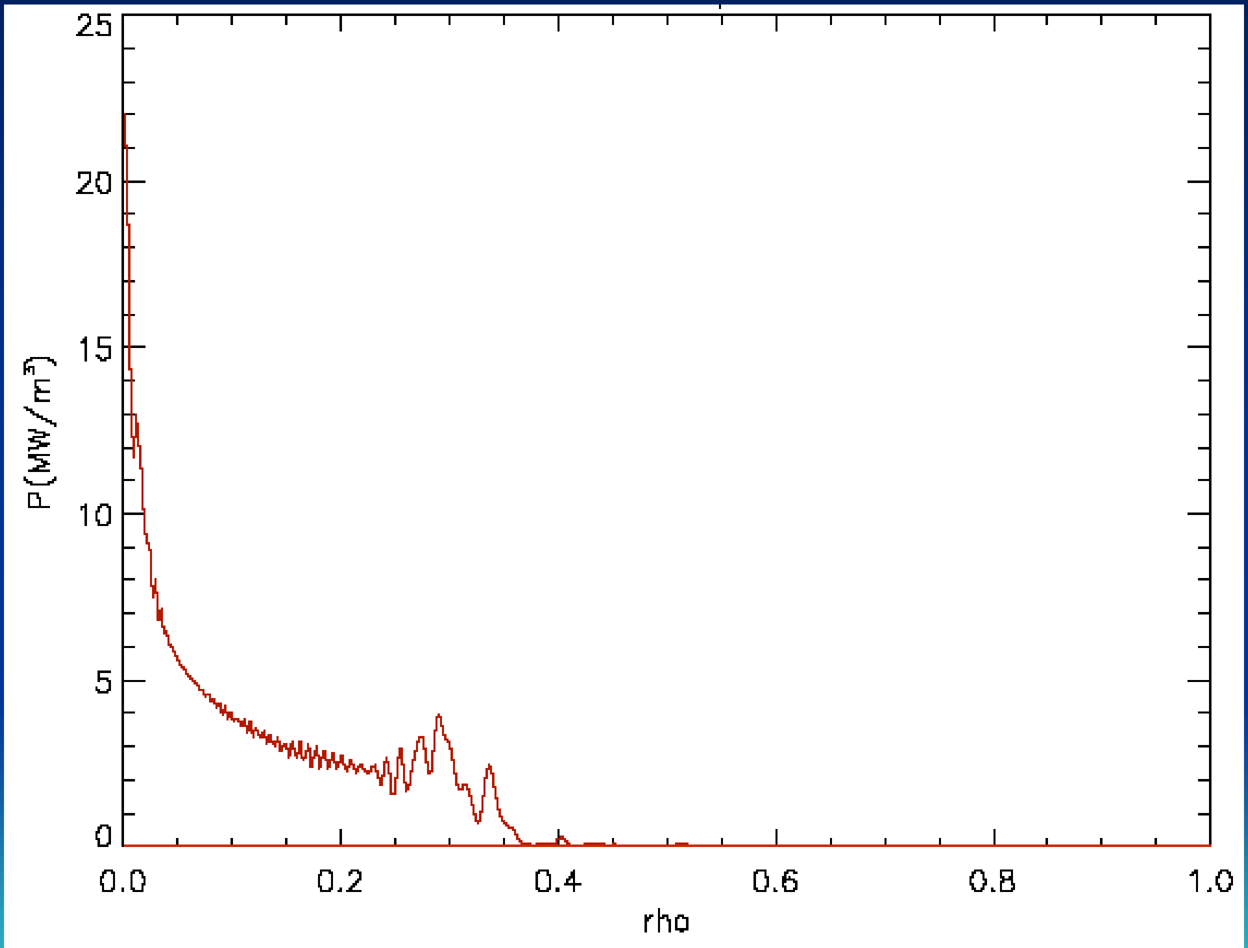

O-X-B modes coupling at EC fundamental harmonic in T-10 like O-mode quasi perpendicular outside launch at $N_e < N_{crit}|_{O\text{-mode}}$, |E_total| no SPA

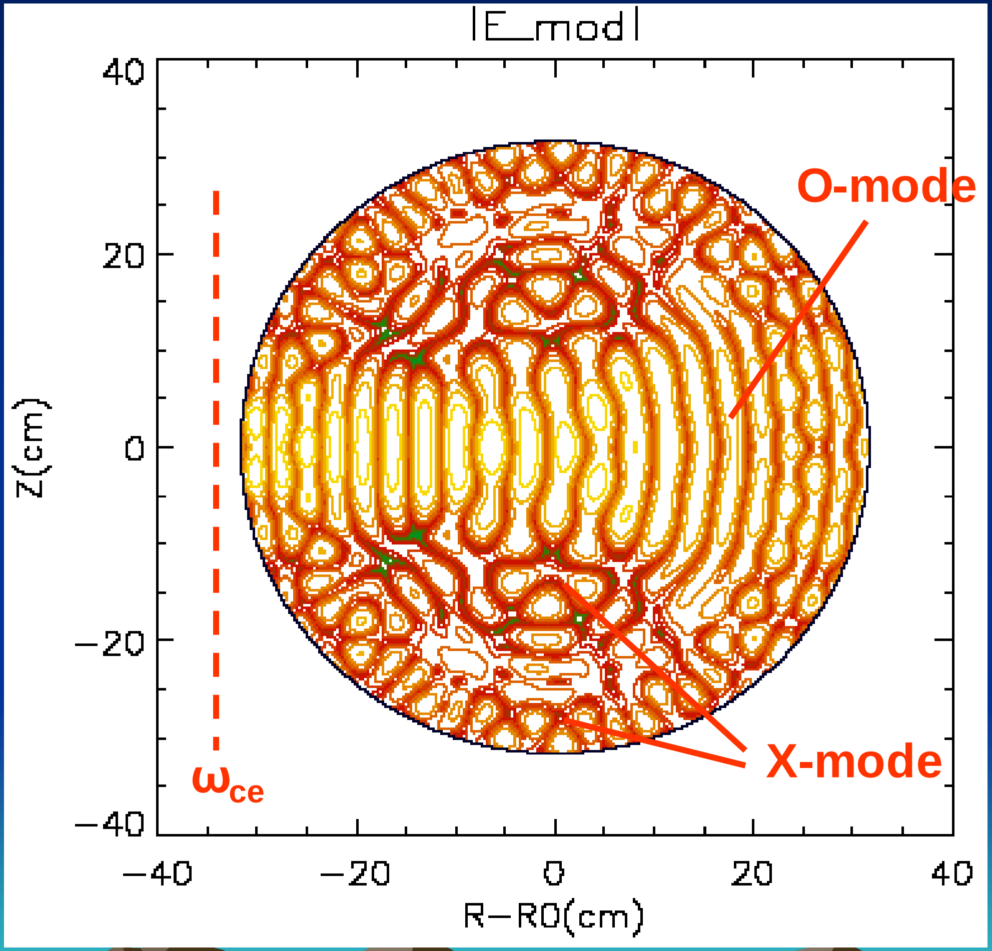

O-X-B modes coupling at EC fundamental harmonic in T-10 like O-mode quasi perpendicular outside launch at $N_e < N_{crit}|_{O\text{-mode}}$, |E_total| - ε_{13} , ε_{23} terms included

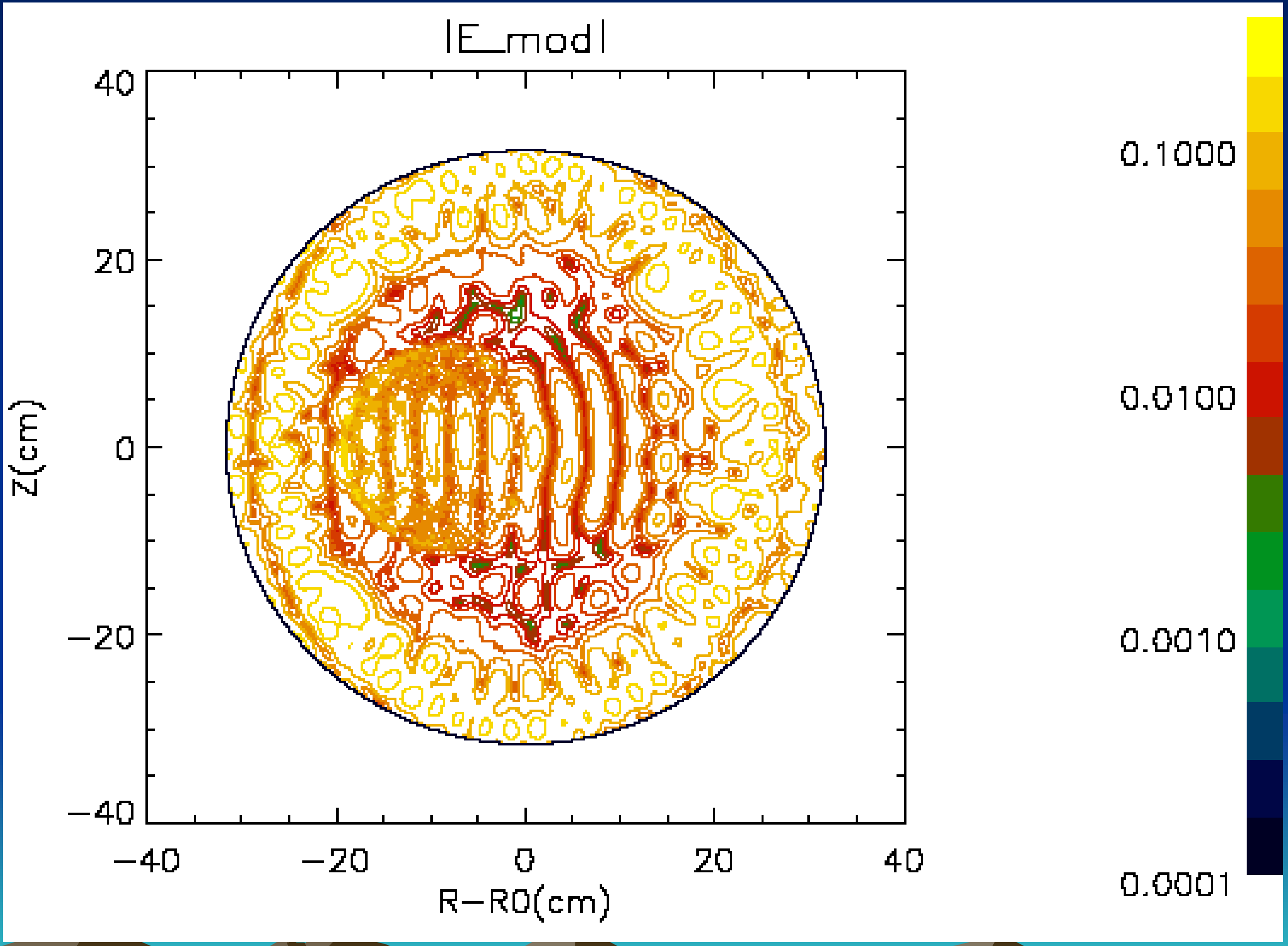

Similar EC heating efficiencies at fundamental harmonic in DIII-D for O-mode and X-mode launches at 60 GHz were reported

- R.Prater et al, ICPP98 poster, Praha (1998)

  1) Nice explanation argued to X-mode reflection from X's cut off and conversion to O-mode during reflection from the walls

  2) Full wave code treats this "conversion" effect automatically and knows something about O or X modes only through antenna polarization

T-10/DIII-D modelling at 60 GHz

- Toroidal field, Bo — 2.14 T
- Plasma current — 0.14-0.28 MA
- Central electron temperature (to increase EBW resolution) — 36.8 keV
- Temperatures exponent, α_T — 2.0
- Central electron density — 2.3×10^{19} m^{-3}
- Separatrix electron density — 2.3×10^{18} m^{-3}
- Density exponent, α_n — 1.0
- RF power — 1 MW
- RF frequency — 60 GHz
- Outside launch $N_{//}(0)$ spectrum — 0.016 – 0.3

O- and X-mode |E_minus| in T-10/DIII-D at 60 GHz, $N_{//}$=0.16

A(X-mode)~7A(O-mode)

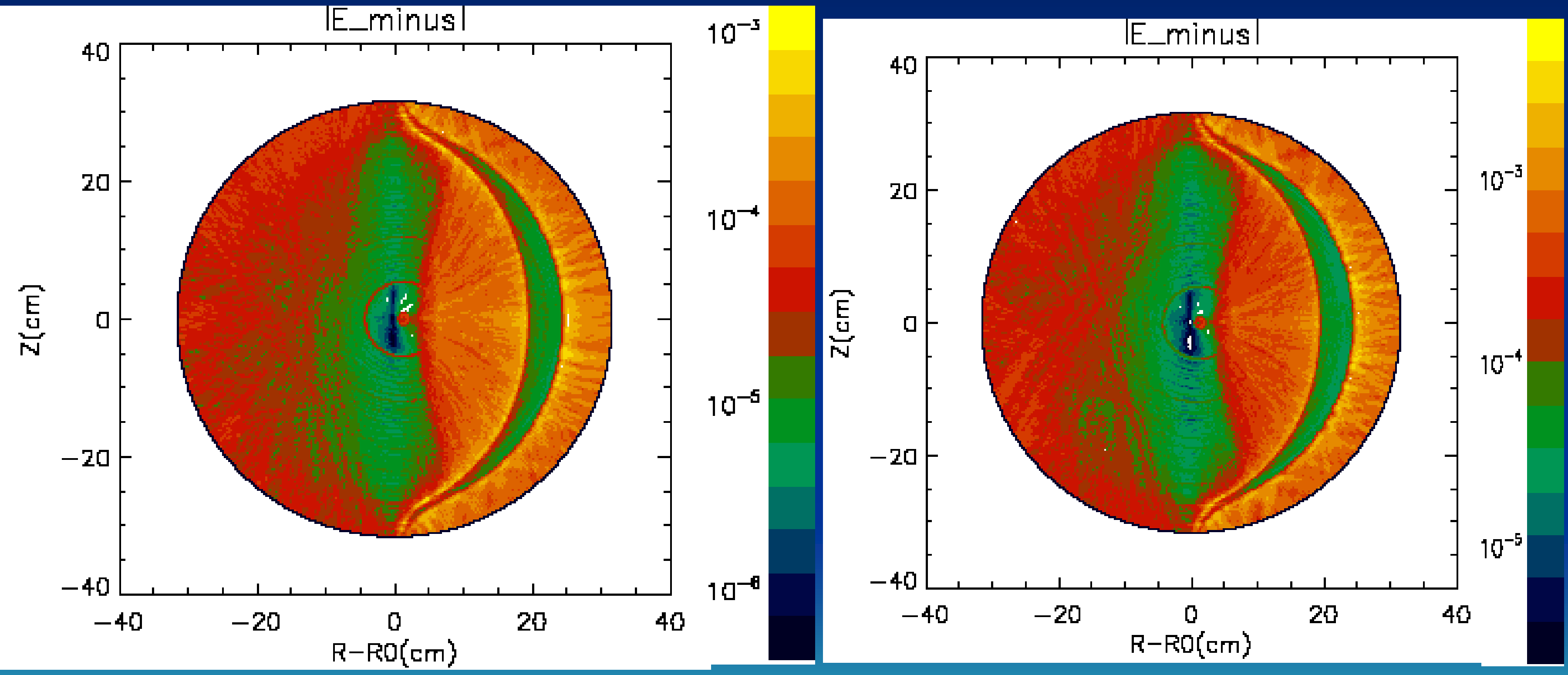

O- and X-mode |Re(E_psi)| in T-10/DIII-D outside launch at 60 GHz, $N_{//}$=0.16

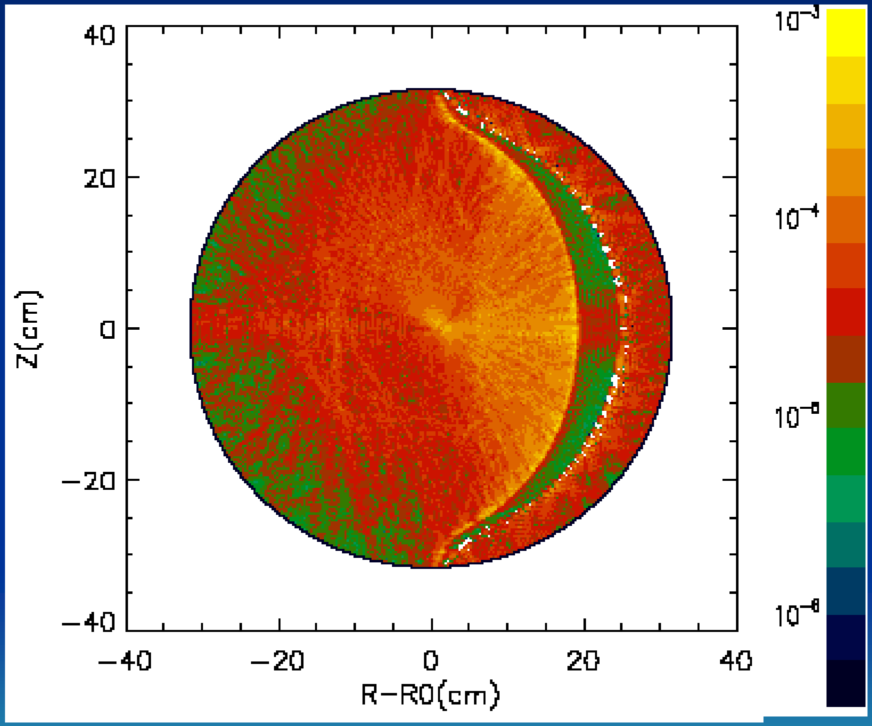

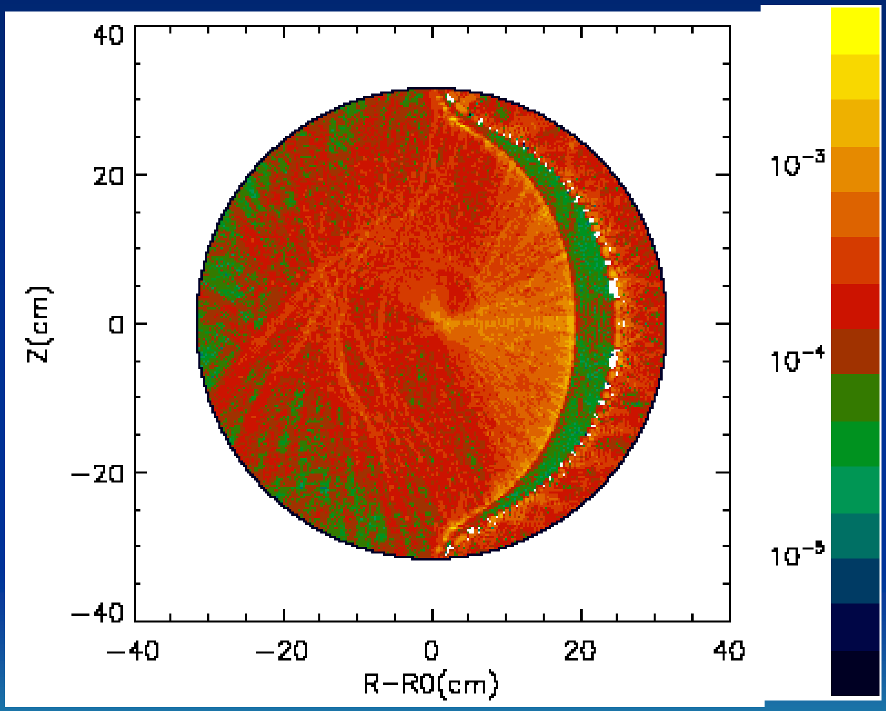

O- and X-mode |Im(E_z)| in T-10/DIII-D at 60 GHz, N//=0.16

O-mode

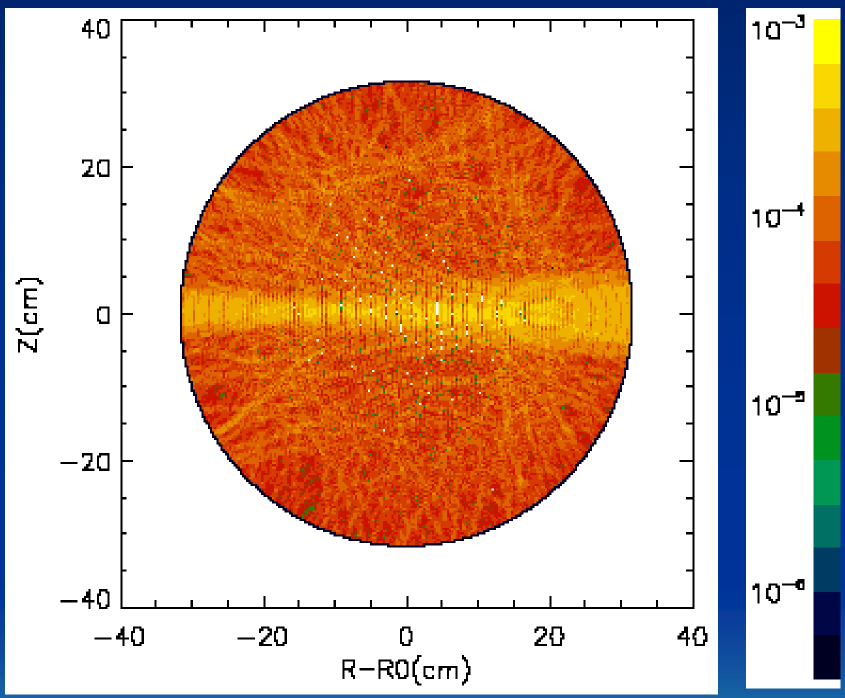

X-mode

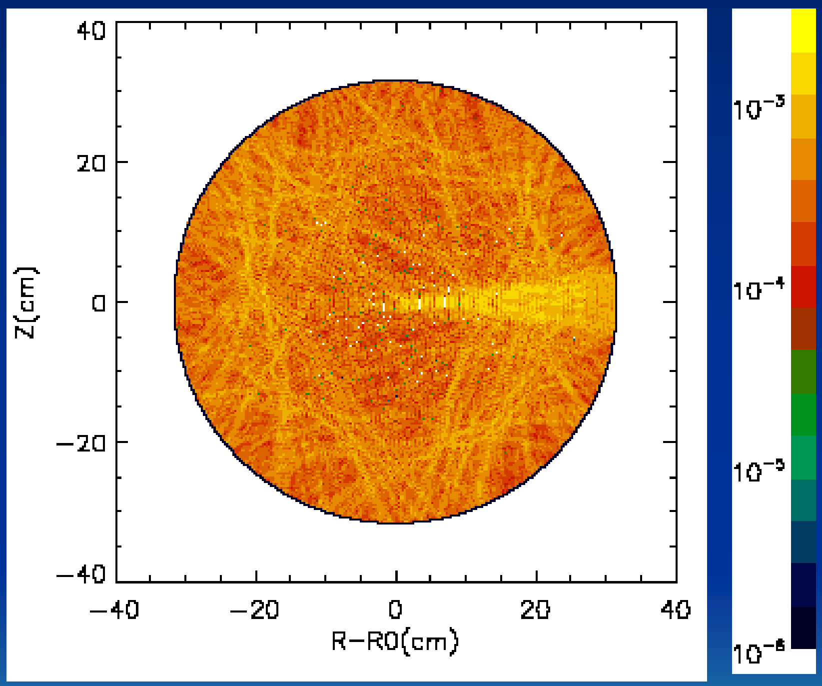

Power deposition for O- and X-mode in T10/DIII-D at 60 GHz, N//=0.16

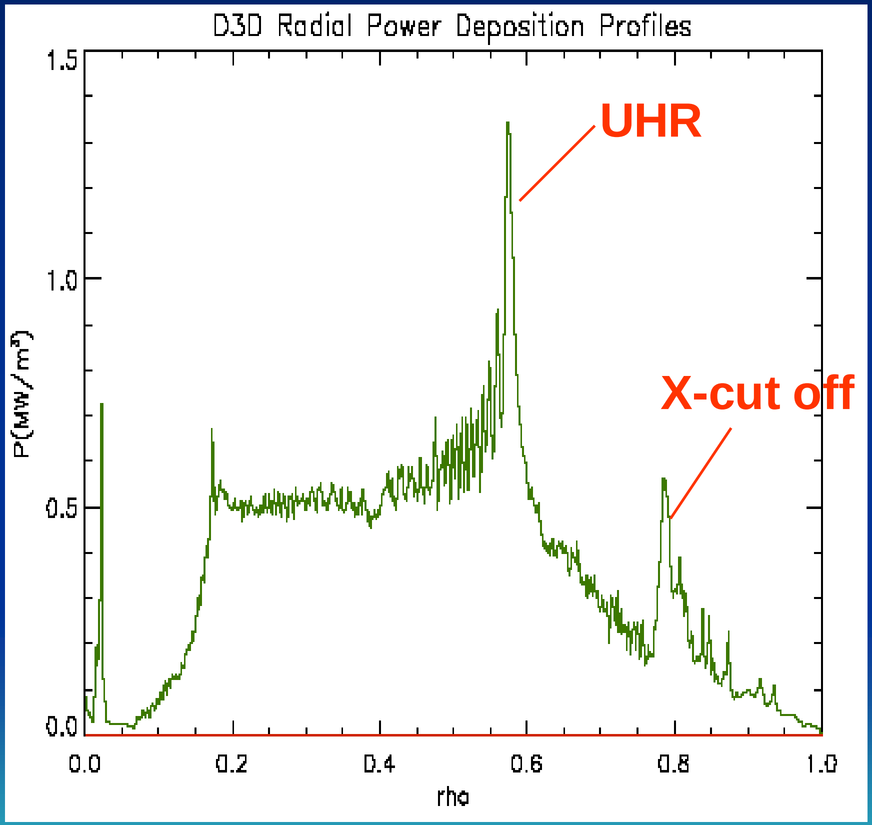

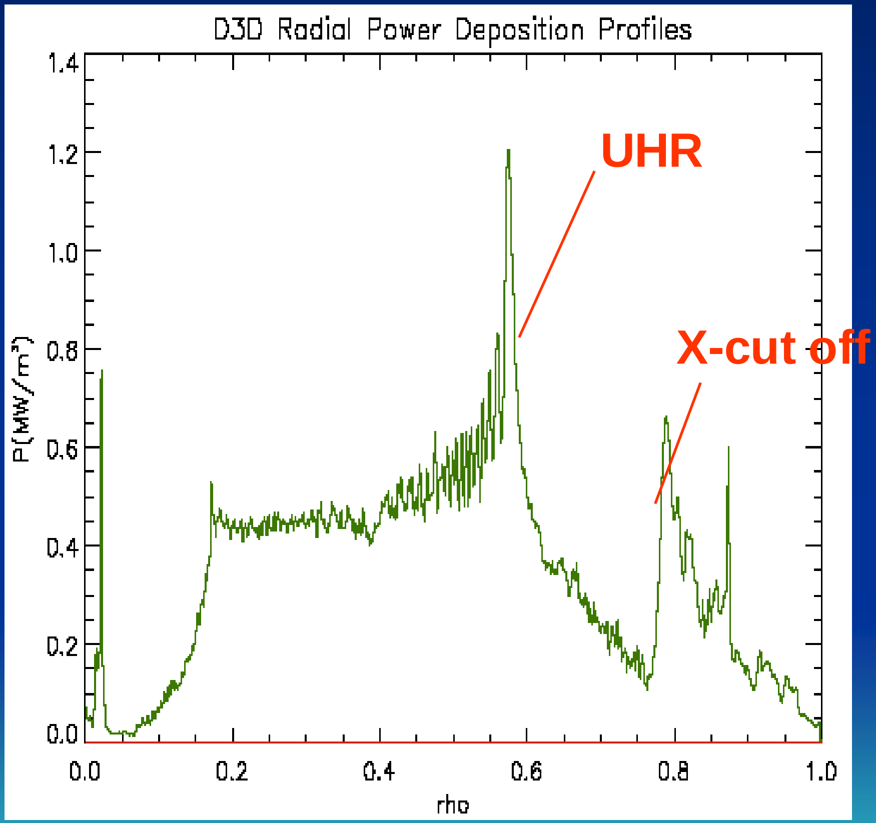

O- and X-mode |re(E_minus)| in T-10/DIII-D at 60 GHz quasi perpenducular launch, $N_{//}$=0.016

A(X-mode)~10A(O-mode)

O-mode **X-mode**

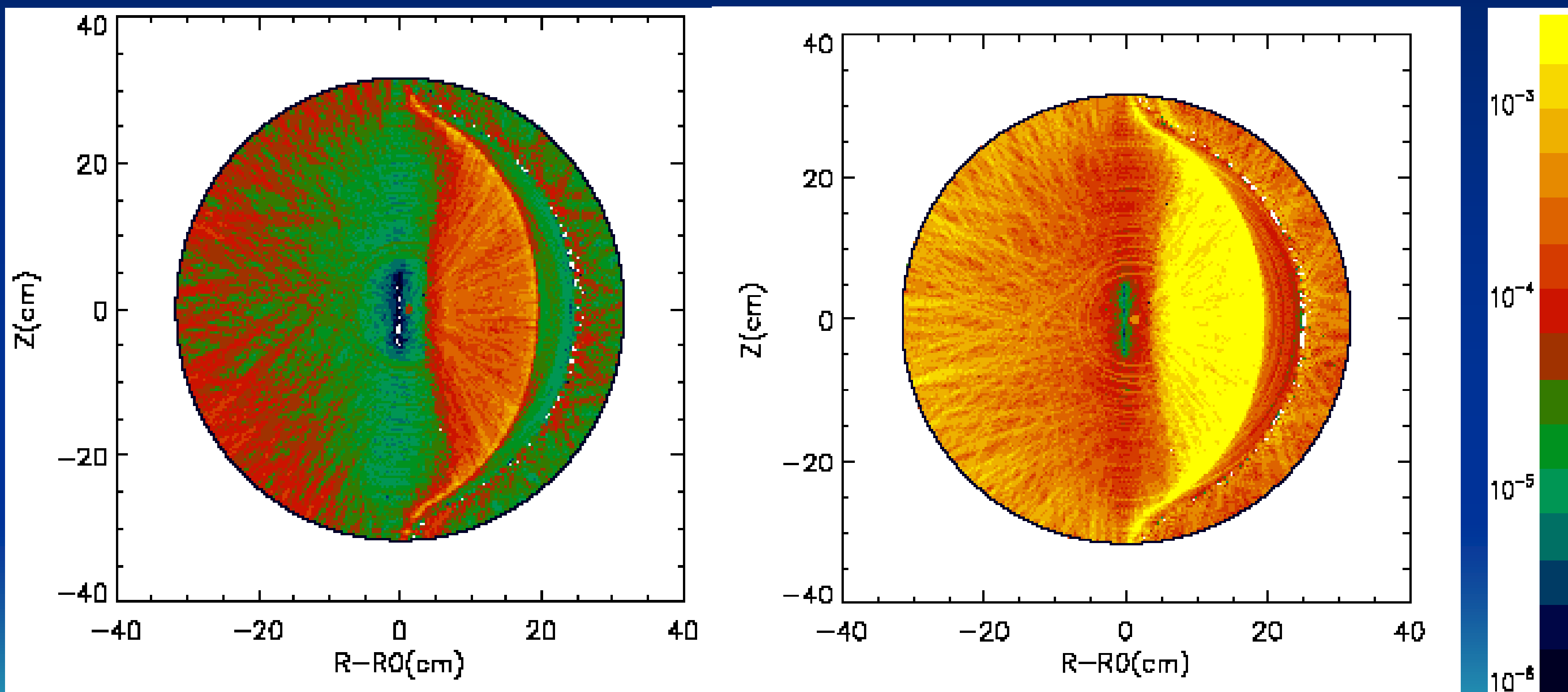

Power deposition for O- and X-mode in T10/DIII-D at 60 GHz $N_{//}$=0.016 are very similar while X-mode excited amplitudes are ~10 times higher of O-mode ones

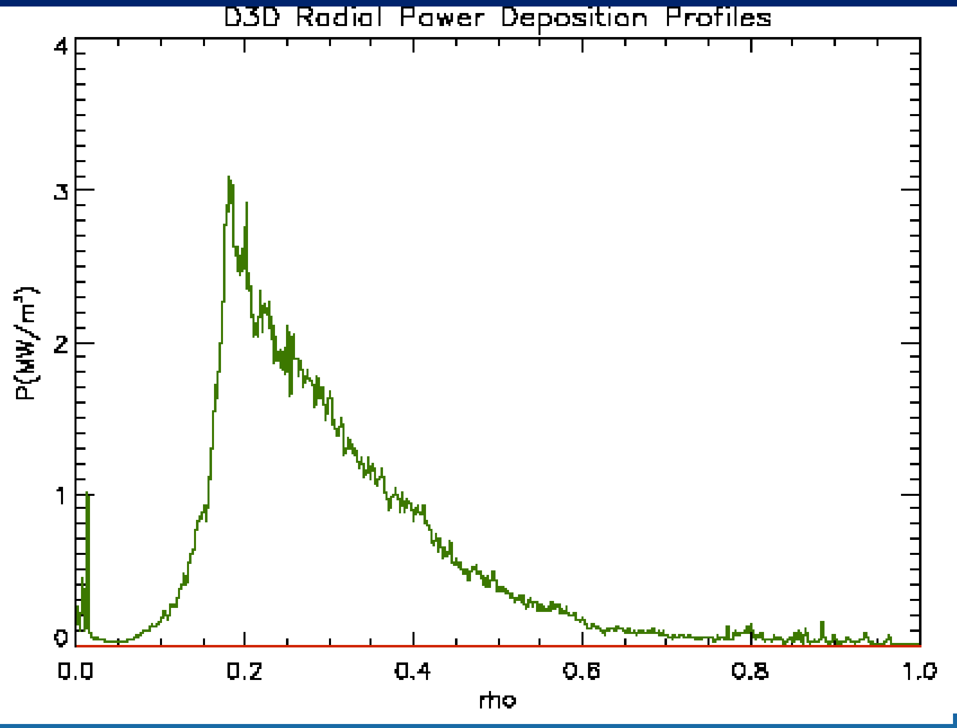

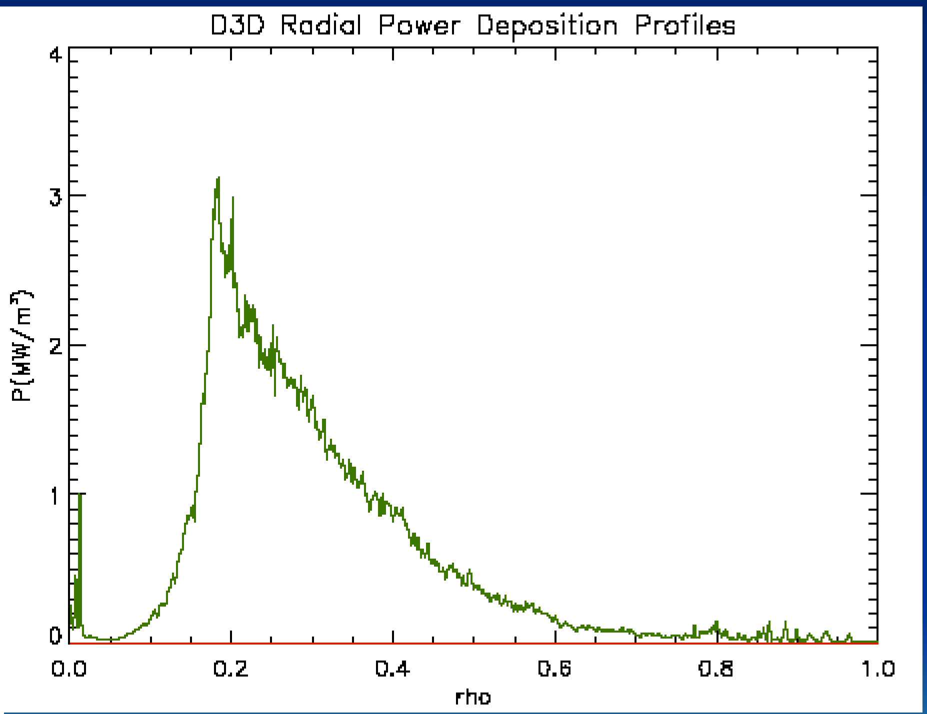

ITER fundamental harmonic modelling at 11.15 GHz

Toroidal field, Bo	0.33-0.39 T
Plasma current	0.634 MA
Central electron temperature	25.8 keV
Temperatures exponent, α_T	1.0
Central electron density	3×10^{17} m^{-3}
Separatrix electron density	3×10^{16} m^{-3}
Density exponent, α_n	1.0
RF power	1 MW
RF frequency	11.15 GHz
Outside launch $N_{//}(0)$ spectrum	0.016 – 0.5

O-mode fundamental harmonic quasi perpendicular equatorial launch at $N_{//}$=0.017, Bo=0.381 T, X(ω_{ce})= -27 cm, X(UHR)=38 cm, |Re(E_minus)|

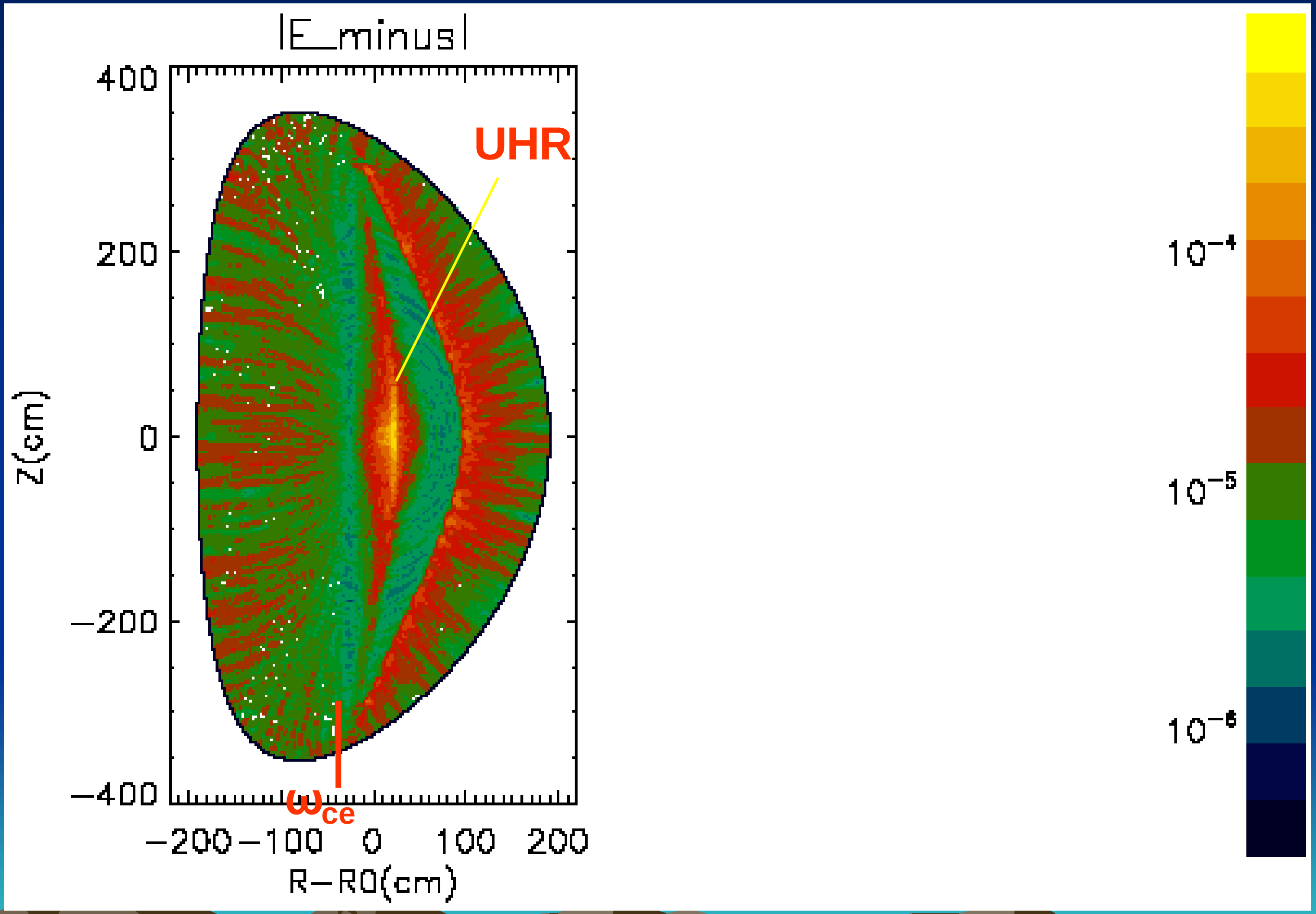

O-mode fundamental harmonic quasi perpendicular equatorial launch at $N_{//}$=0.017, Bo=0.381 T, Radial power deposition P(rho)

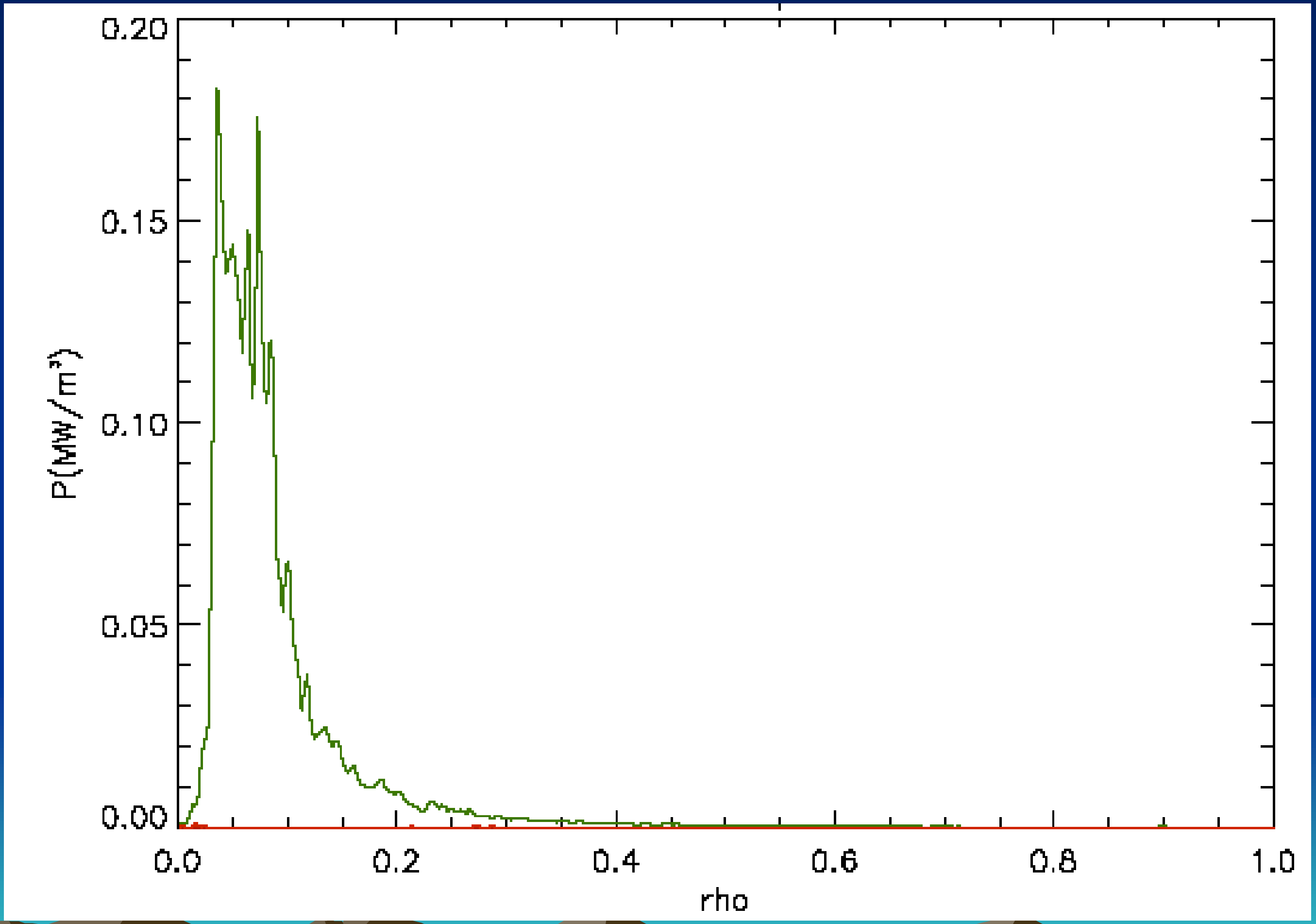

O-mode fundamental harmonic quasi perpendicular equatorial launch at $N_{//}$=0.017, Bo=0.361 T, Radial power deposition P(rho) (cold resonance at rho=0.35)

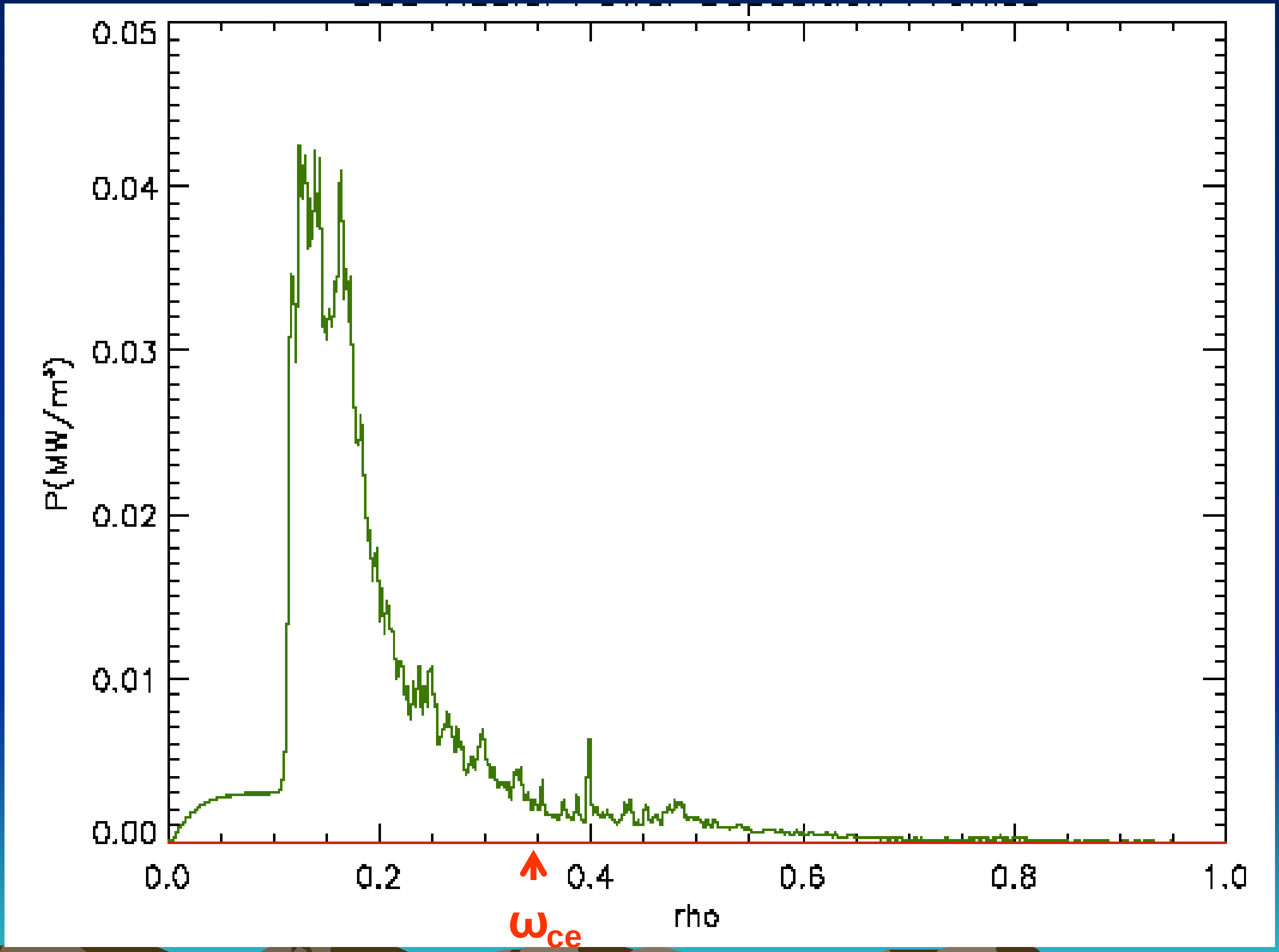

O-mode fundamental harmonic oblique outside launch at $N_{//}$=0.49, Bo=0.391 T, efficient mode conversion to EBW X(ω_{ce})= -11 cm, X(UHR)=53.5 cm, |E_minus|

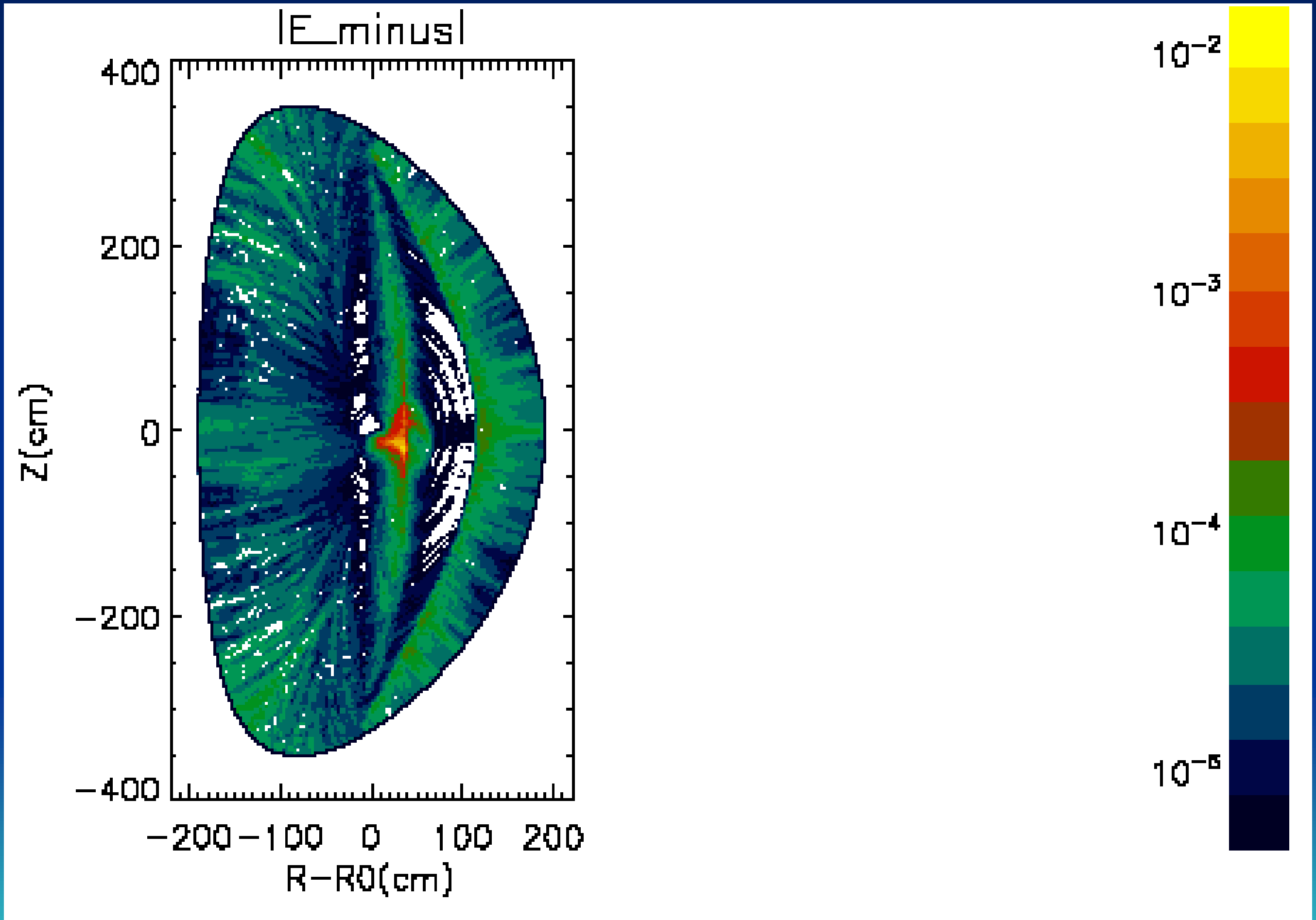

O-mode fundamental harmonic oblique outside launch at $N_{//}$=0.49, Bo=0.391 T,

Radial power deposition P(rho) (cold resonance at rho=0.108)

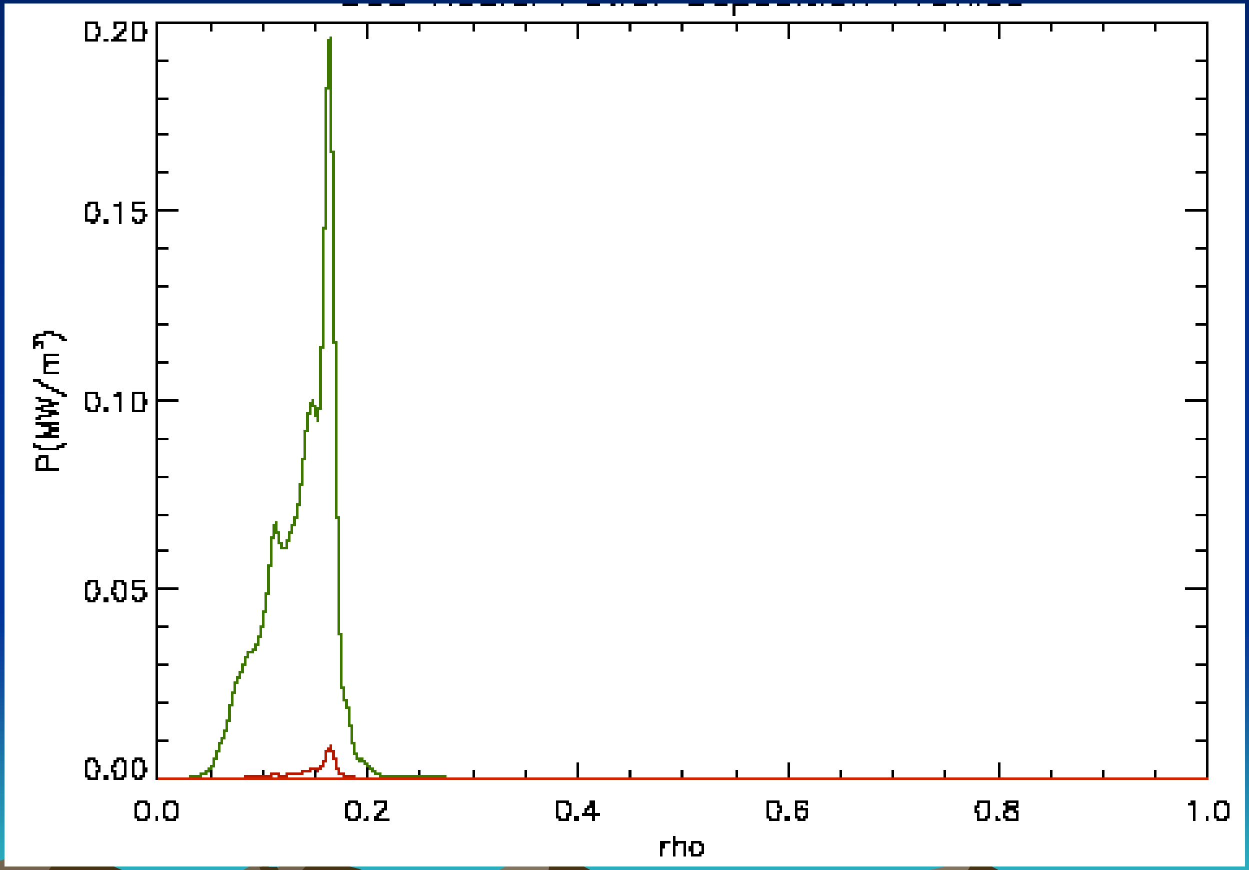

O-mode fundamental harmonic oblique outside launch at $N_{//}$=0.49, Bo=0.391 T, X(ω_{ce})= -11 cm, X(UHR)=53.5 cm,

|Im(E_z)|, EBW are: 1) crucial in power deposition location 2) EBW interact with very energetic electrons – CD rises

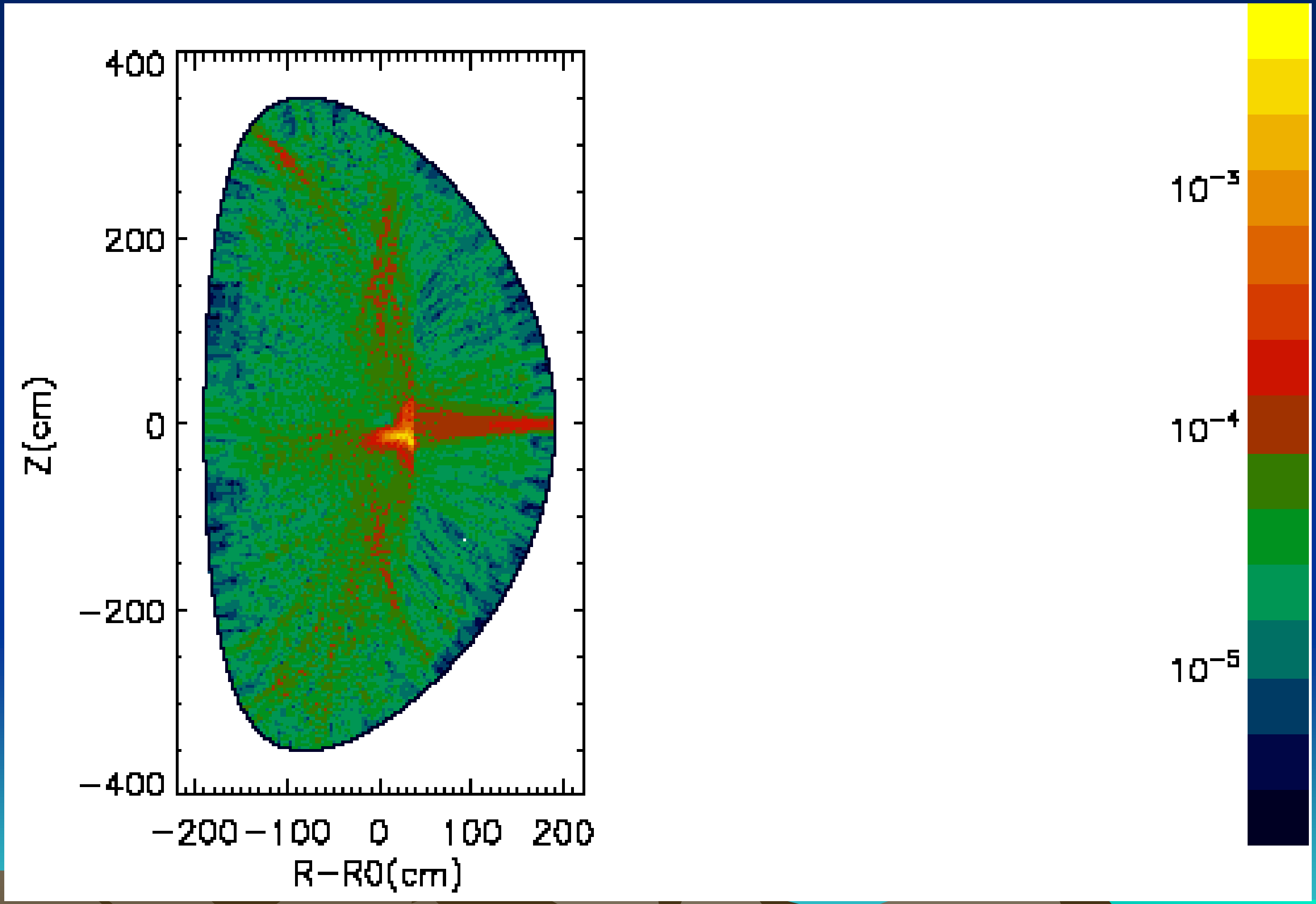

Second harmonic ECRF modelling

- Second harmonic X-mode scenario
  in T-10, DIII-D, JET, TCV and ITER
  - usually No Upper Hybrid resonance
  - interplay of refraction, reflection, interference and diffraction
  - decreased density cut offs
  - similarity laws check for ITER

Coupling X-mode and O-mode, 2 diffraction lobs

Second harmonic X-mode upper port launch at **F=60 GHz** in DIII-D H-mode: |real(E_eps)|, |Im(E_z)|

N=160 ($N_{//}(0)$=0.075), T_{e0}=6.55 kV Ne(0)=1.0×10^{19} m^{-3} I_p=360 kA

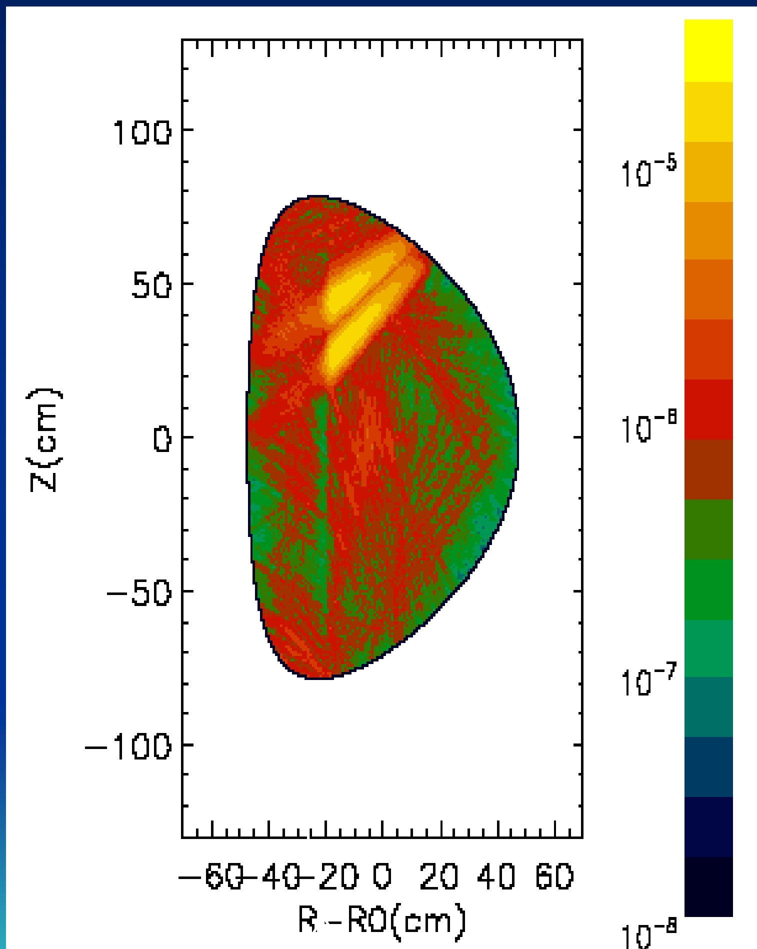

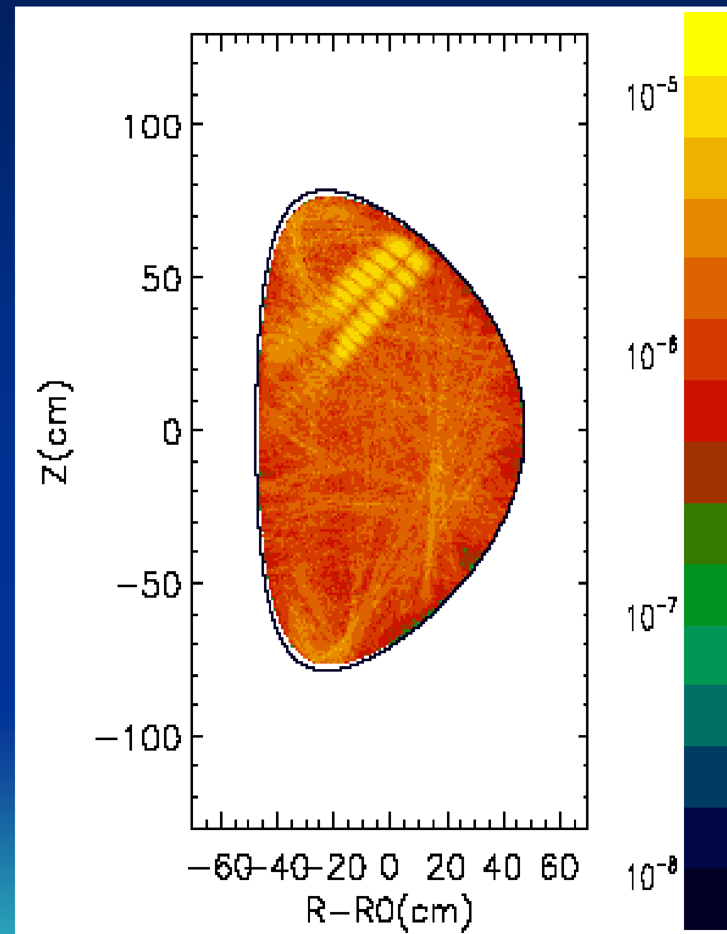

$\Omega=2\omega_{ce}$

Second harmonic X-mode launch in DIII-D H-mode plasma: Radial power deposition to electrons, two diffraction lobs

N=160 ($N_{//}(0)$ = 0.075), F=60GHz, Ne(0)=1.0×10^{19} m^{-3} I_p=360 kA

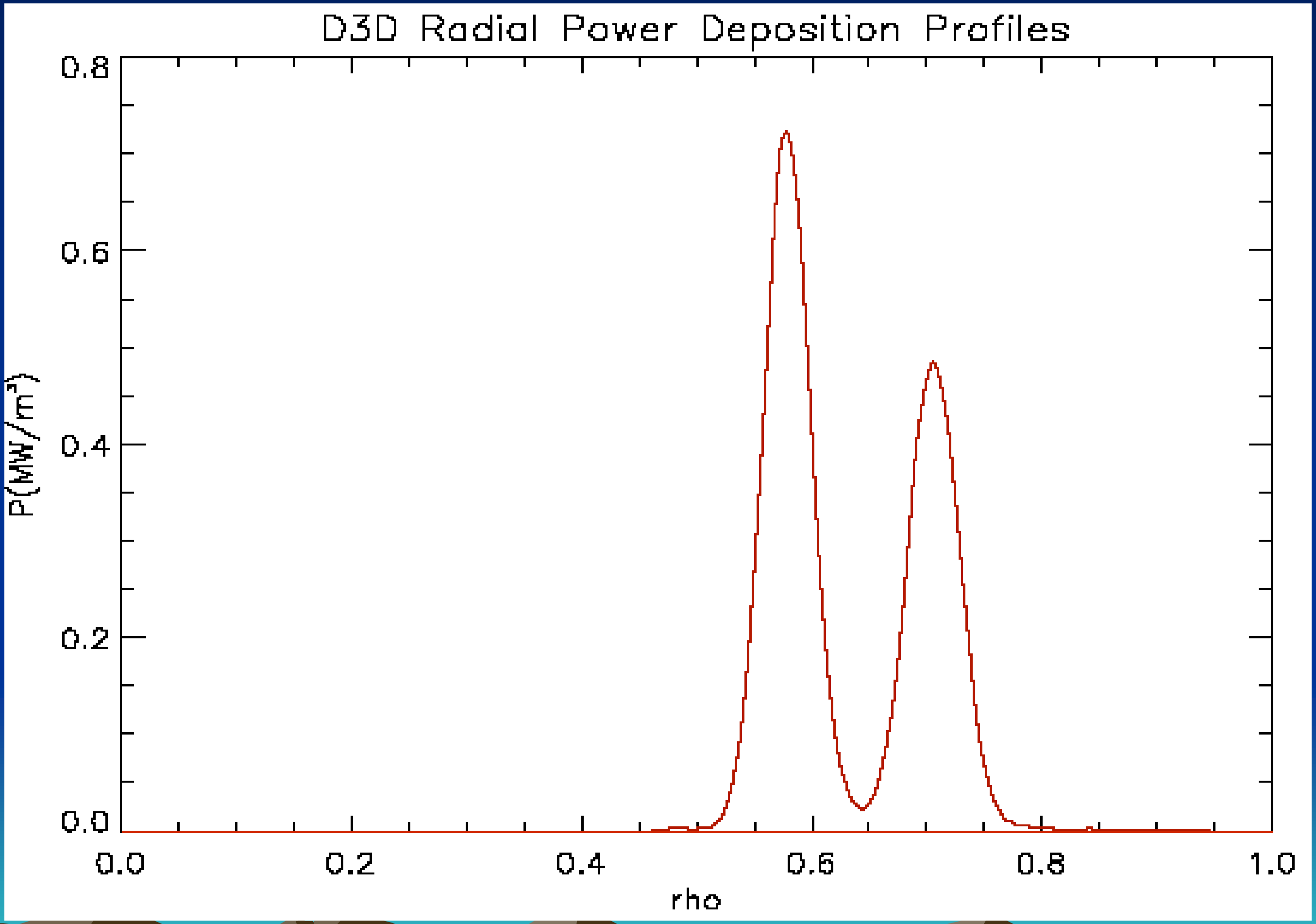

At lower density coupling X-mode and O-mode is weaker

Second harmonic X-mode upper port launch at

F=60 GHz in DIII-D L-mode: |real(E_eps)|, |Im(E_z)|

N=160 ($N_{//}(0)$=0.075), T_{e0}=6.55 kV Ne(0)=0.5×10^{19} m^{-3} I_p=360 kA

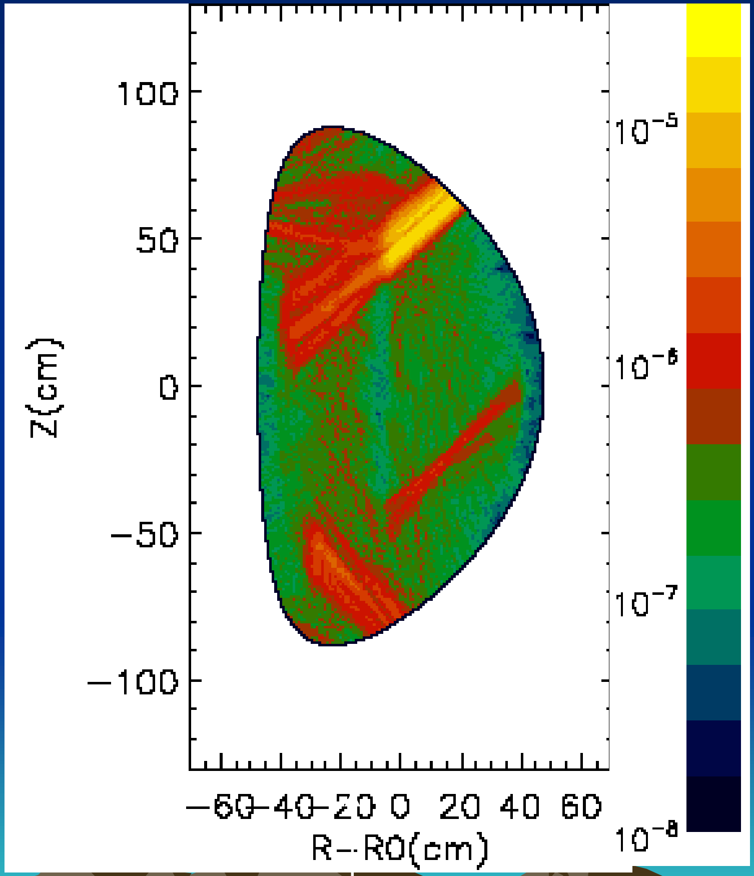

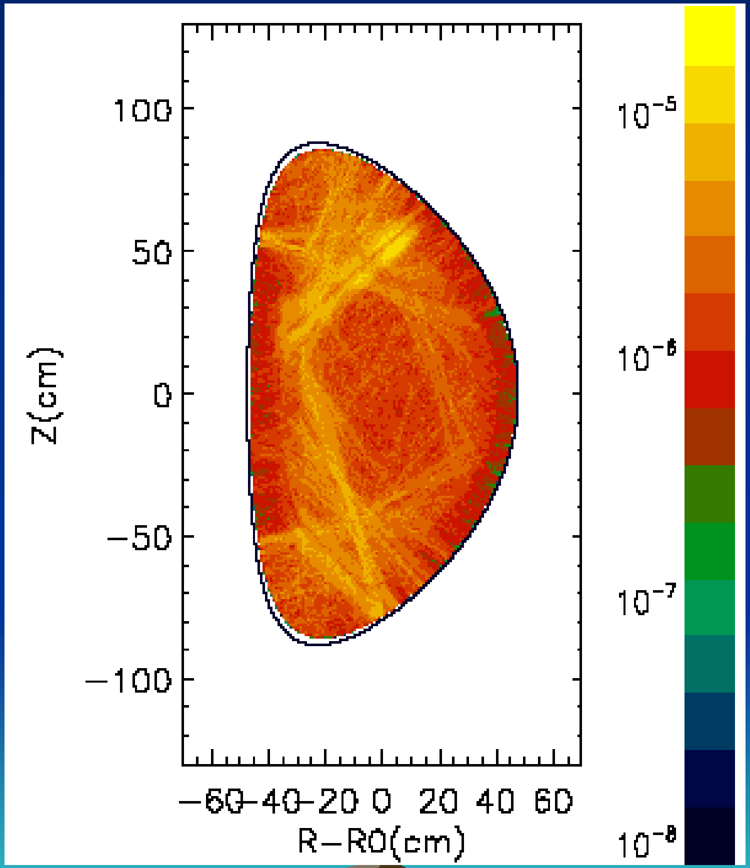

$\Omega=2\omega_{ce}$

Second harmonic X-mode launch in DIII-D L-mode
more density rare and smooth plasma:
Radial power deposition to electrons, two diffraction lobs

$N=160$ ($N_{//}(0) = 0.075$), $F=60GHz$, $Ne(0)=0.5\times10^{19}\ m^{-3}$ $I_p=360\ kA$

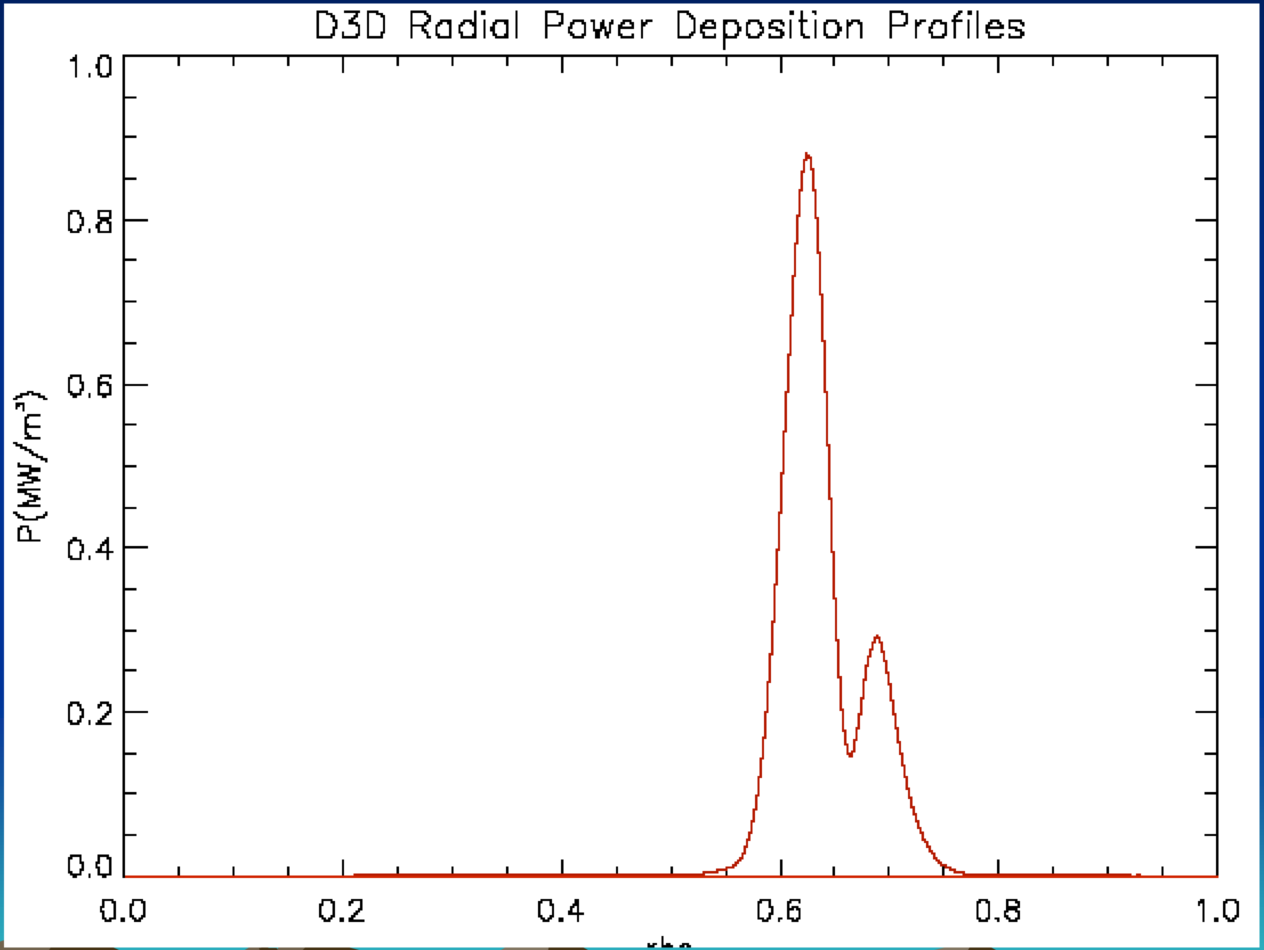

Coupling X-mode and O-mode in DENSE DIII-D plasma

$N(0) \sim N_{cr.}$ Second harmonic X-mode upper port launch at **F=60 GHz** in DIII-D L-mode: |real(E_eps)|, |Im(E_z)|

N=160 ($N_{//}(0)$=0.075), T_{e0}=6.55 kV Ne(0)=2.0×10^{19} m^{-3} I_p=360 kA

|real(E_eps)|,

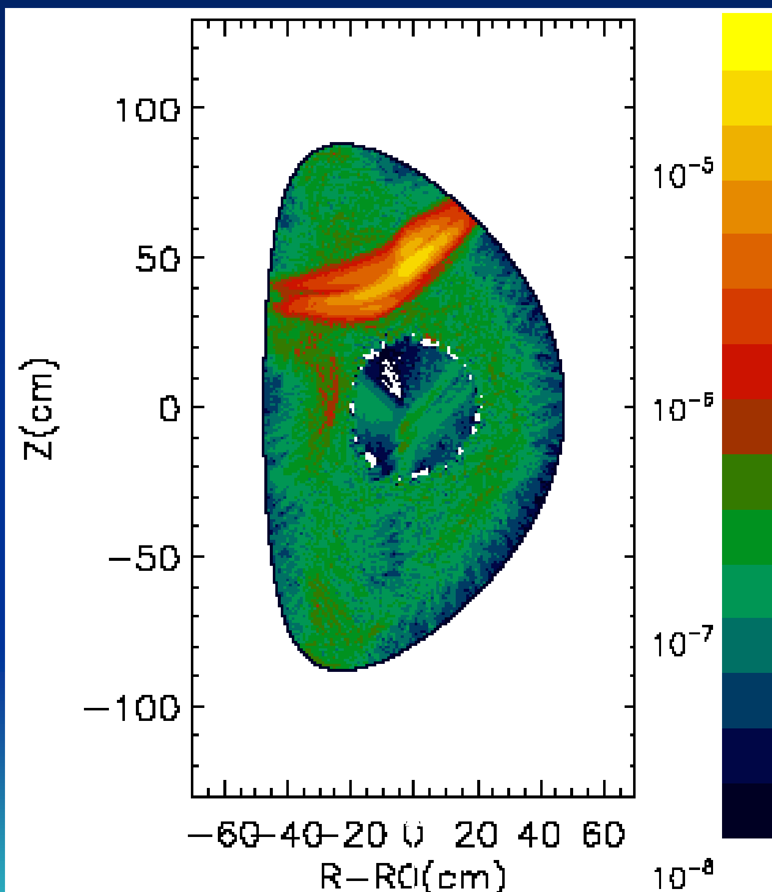

|Im(E_z)|

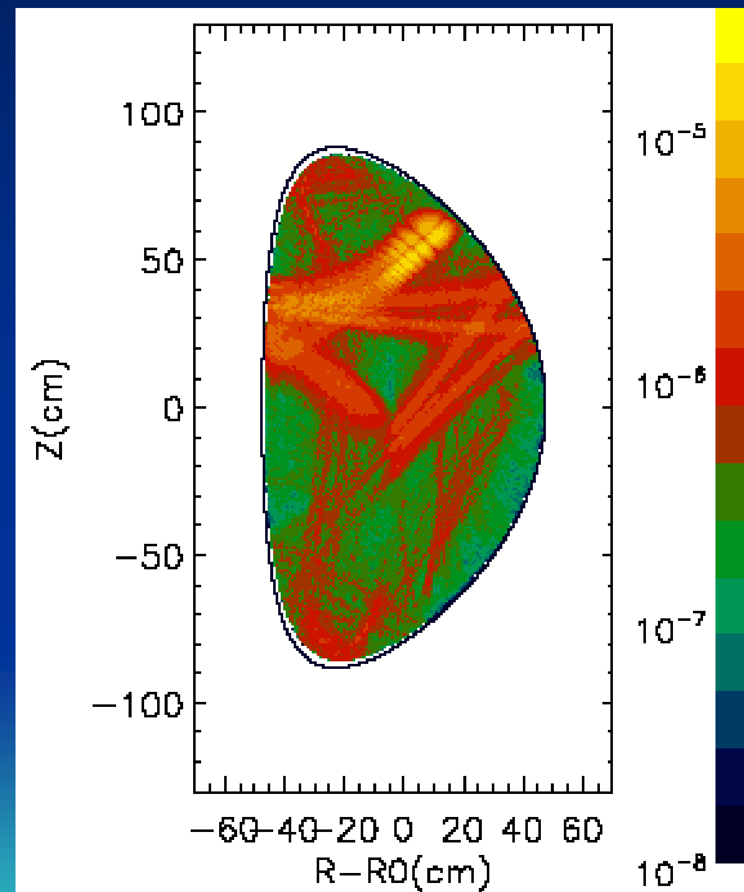

$\Omega=2\omega_{ce}$

Second harmonic X-mode launch in DIII-D L-mode more DENSE plasma case:

Radial power deposition to electrons, three diffraction lobs

N=240 ($N_{//}(0)$ = 0.11), F=60GHz, Ne(0)=2.0×10^{19} m^{-3} I_p=360 kA

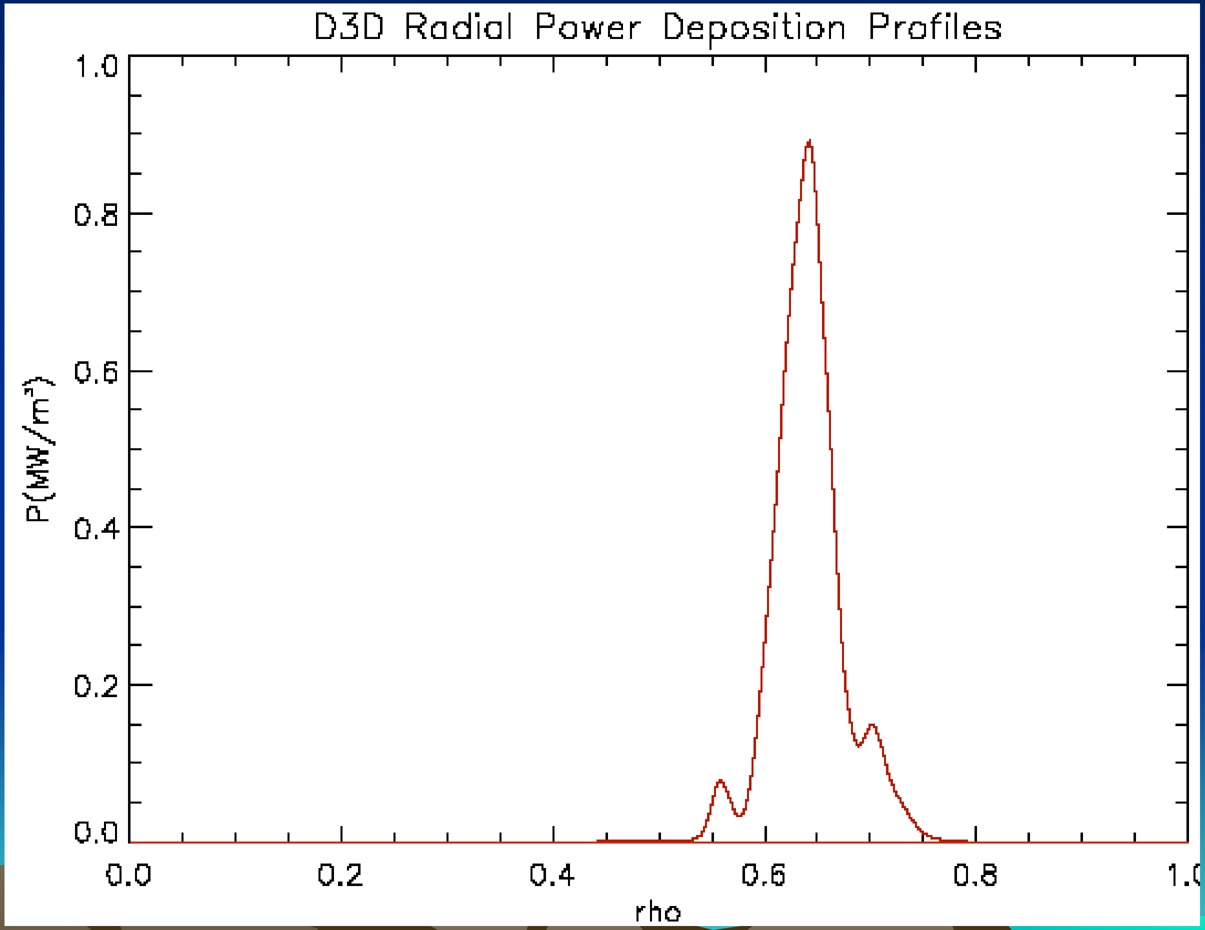

JET ECH second harmonic X-mode

outside quasi perpendicular launch to dense plasma

$F=55$ GHz, $N_{//}(0)=0.0165$ $N_e=1.1\ 10^{19}\ m^{-3}$ |Re(E_psi)|

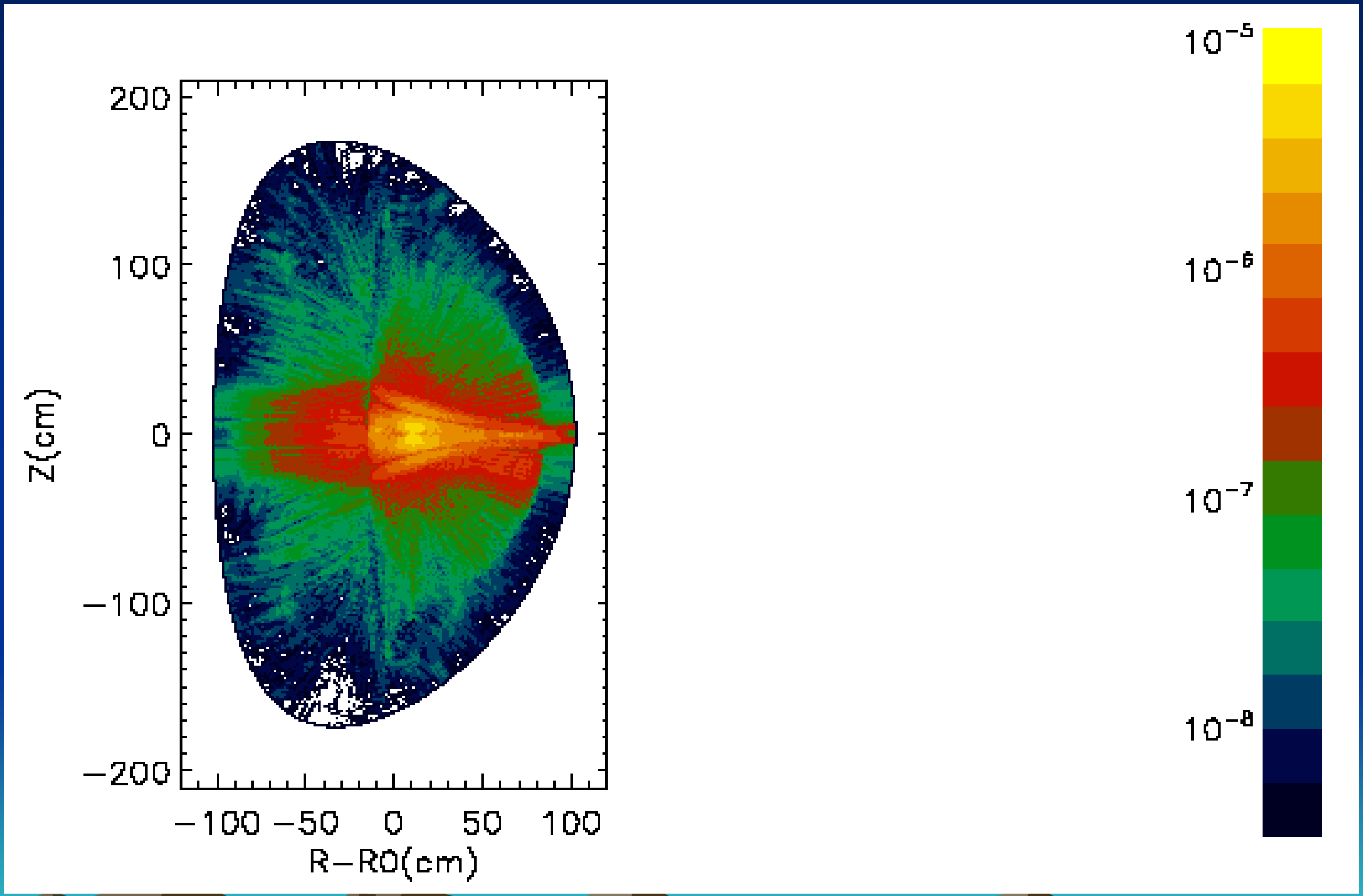

Radial power deposition at X-mode second harmonic equatorial quasi perpendicular launch in JET, $N_{//}$=0.0165

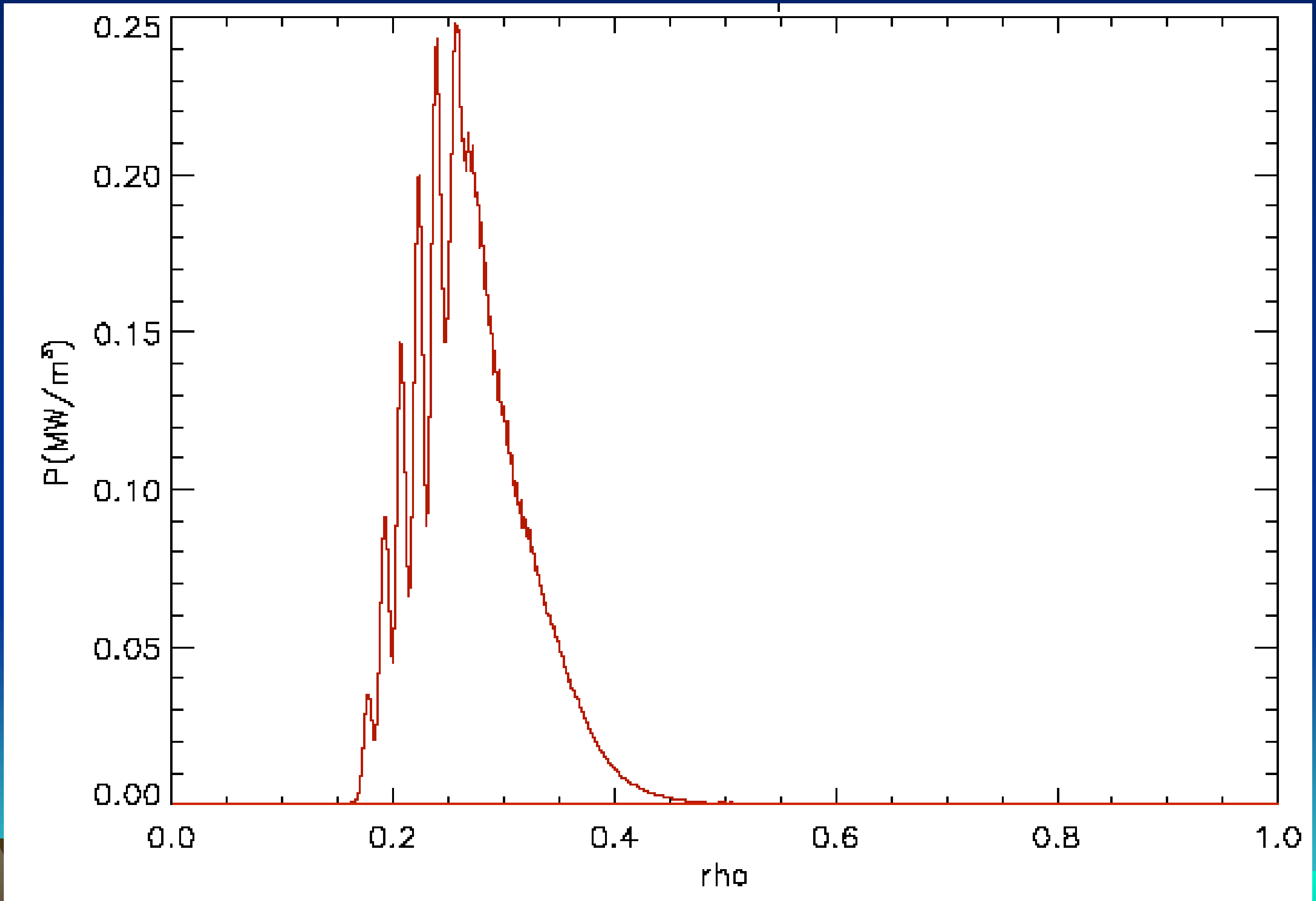

JET ECH second harmonic O-mode outside equatorial launch

F=55 GHz, $N_{//}(0)$=0.2, N_e=1.1 10^{19} m^{-3}, Te(0)=9.8 keV, |Re(E_)|

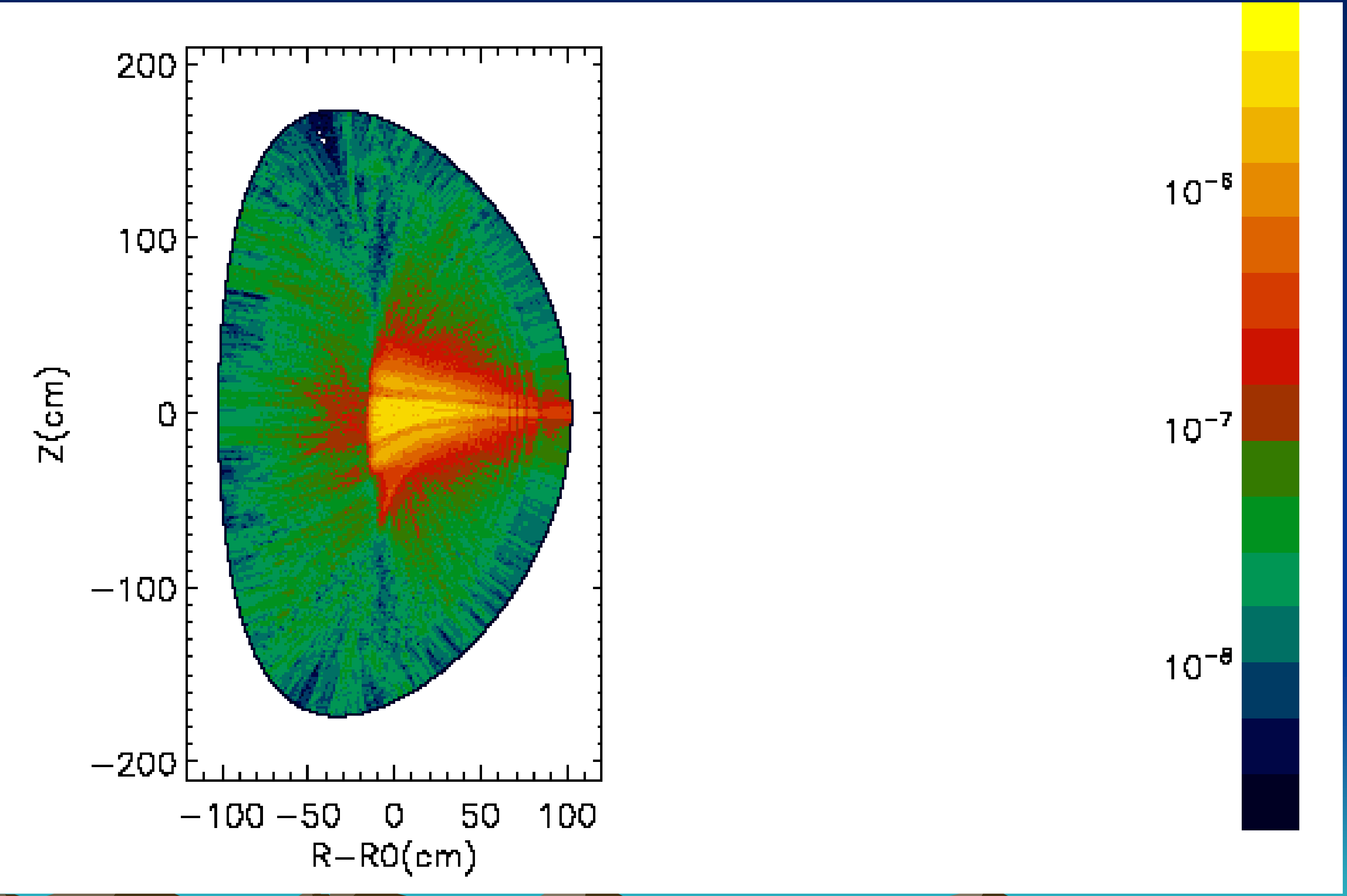

Radial power deposition at O-mode second harmonic equatorial launch $N_{//}=0.2$

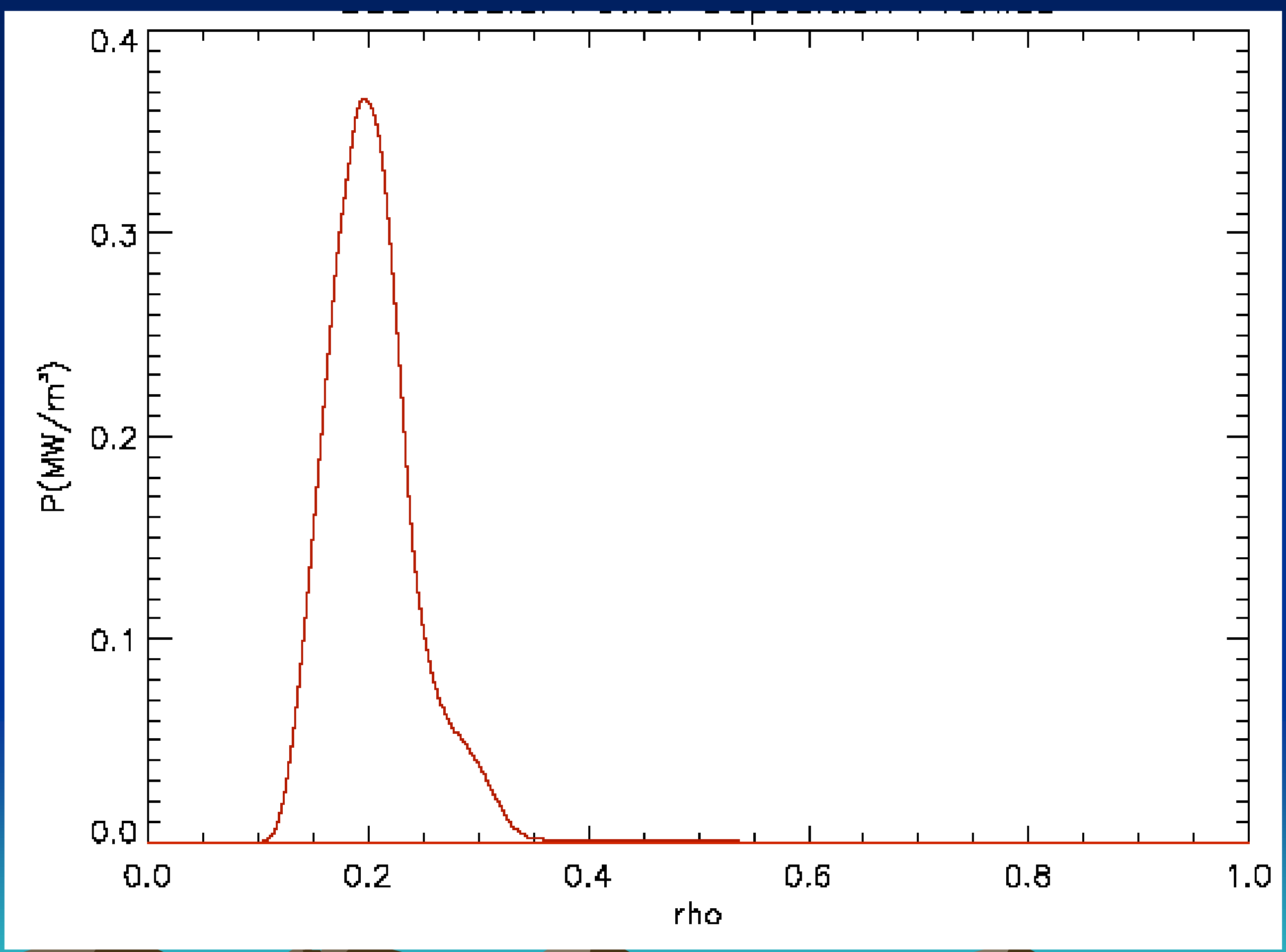

JET ECH second harmonic X-mode outside equatorial $T_e(0)$ = 9.8 keV launch to over dense X-mode plasma

$N(0) = 5\ 10^{18}\ m^{-3}$ F=27.5 GHz, $N_{//}(0)=0.2$

|Re(E_psi)| |Im(E_z)|

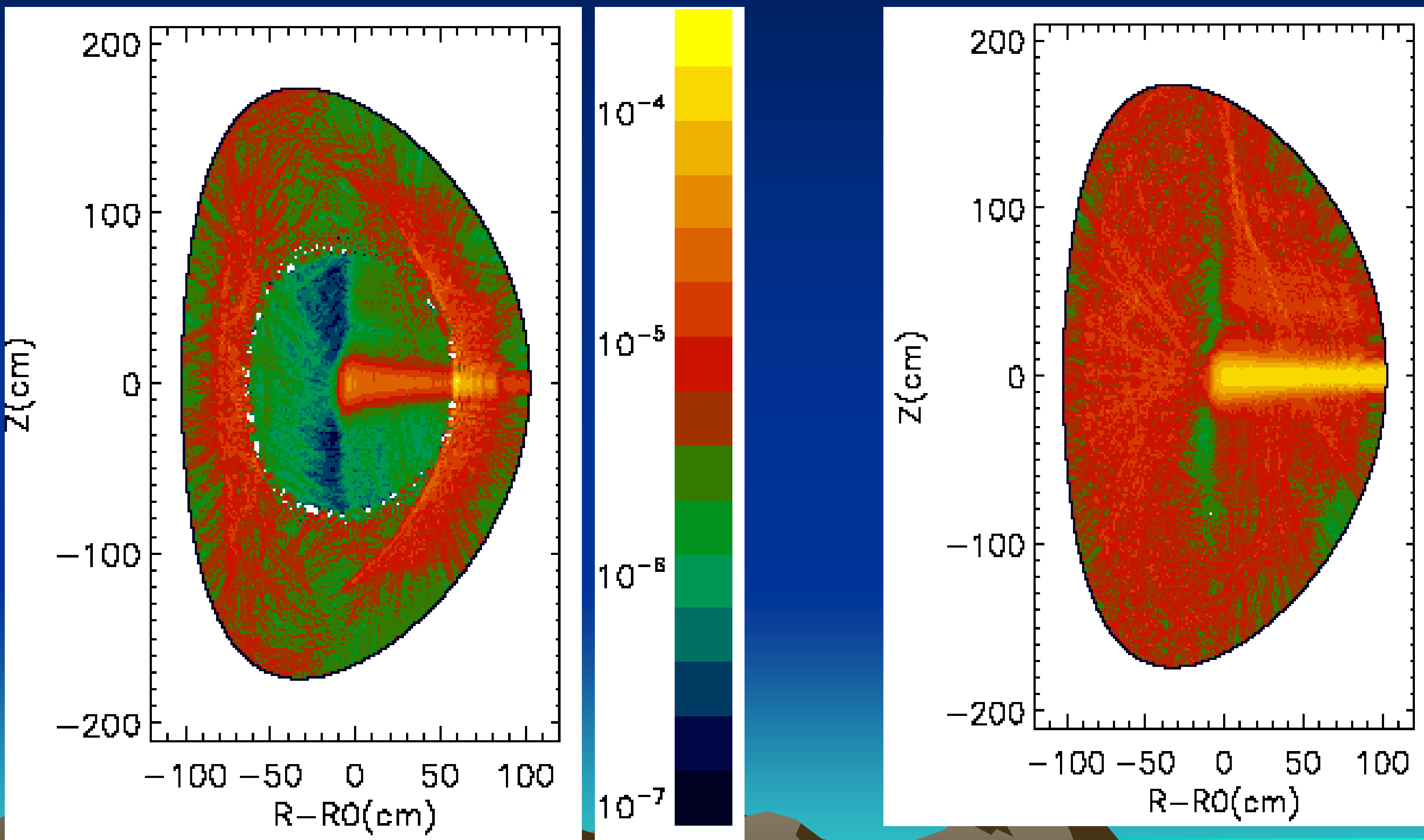

JET ECH second harmonic X-mode outside equatorial

N(0)= 5 10^{18} m^{-3} T(0) = 9.8 keV launch, F=27.5 GHz, $N_{//}(0)$=0.2

Two peaks power deposition from coupled X and O-modes

For X-mode the plasma is over dense one

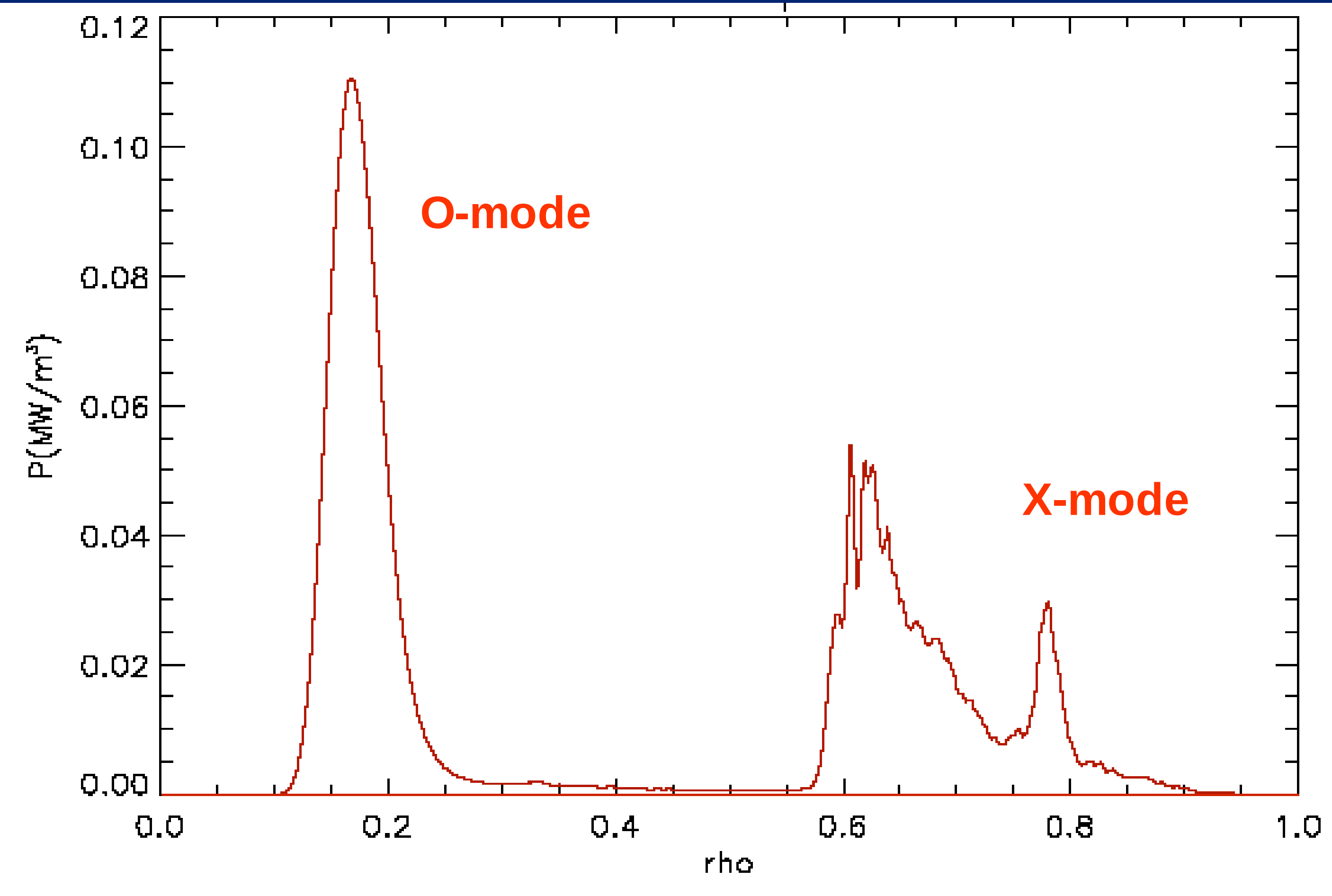

Spherical (A=2) IPHT tokamak ECH second harmonic X-mode outside oblique port launch to H-mode plasma

|(E_minus)| at F=110 GHz, B_o=1.75T, I_p=0.9 MA, $N_{//}(0)$=0.06, N_e=4x 10^{19} m^{-3}, Te(0)=4.9 keV, α_n=0.15, α_T=1.0, SPA regime

|Re(E_minus)|

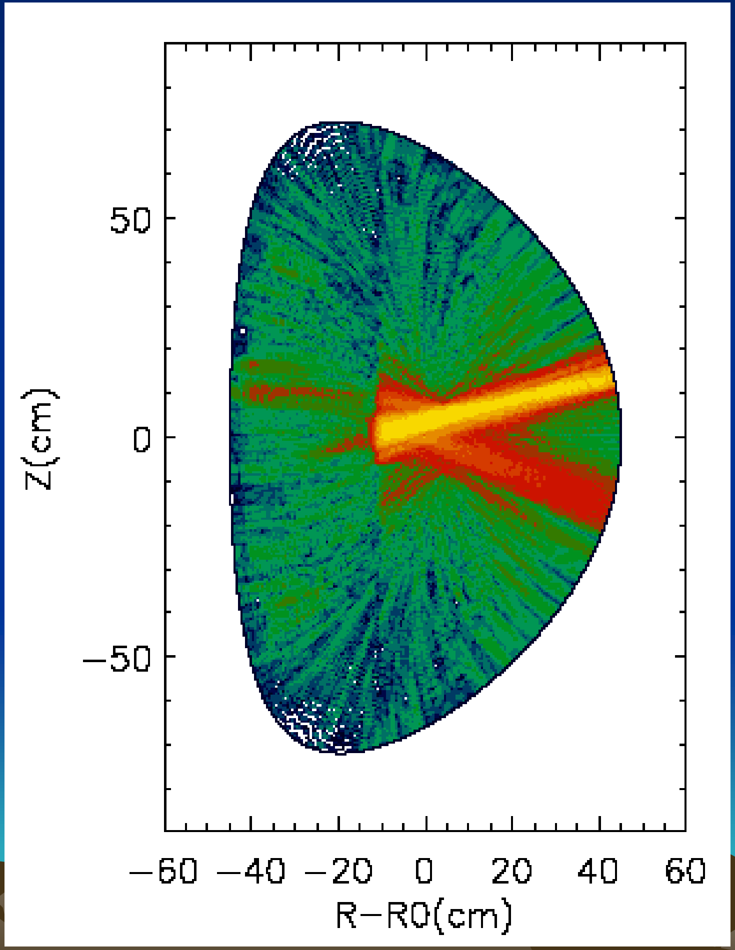

|Re(E_psi)|

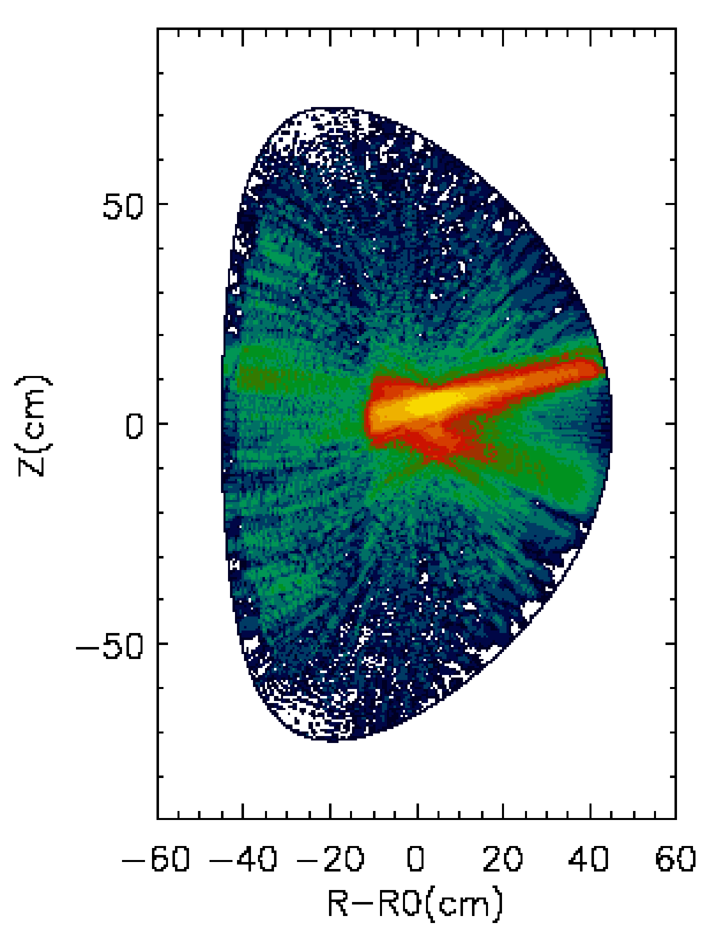

TIN ECH Radial power deposition at X-mode second harmonic oblique outside launch $X(2\omega_{ce}) = -11$ cm, $\Delta|_{Shafr} = 5$ cm

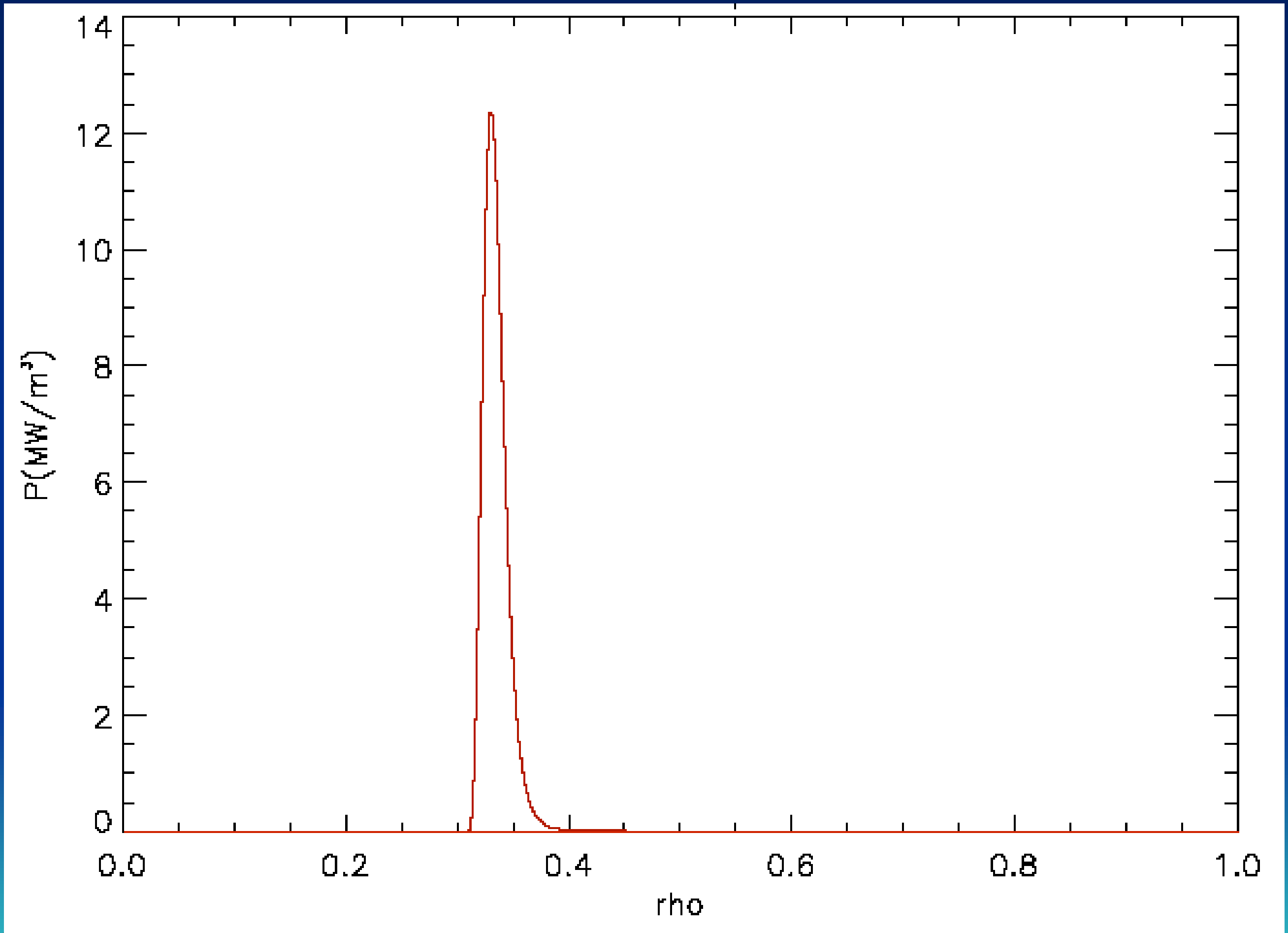

IPHT tokamak ECH second harmonic X-mode

outside oblique port launch to dense H-mode plasma

|(E_minus)| at F=110 GHz, B_o=1.75T, I_p=0.9 MA, $N_{//}(0)$=0.06, N_e=6.5x 10^{19} m^{-3}, Te(0)=4.9 keV, α_n=0.15, α_T=1.0, SPA regime

|Re(E_minus)| **X-cut off**

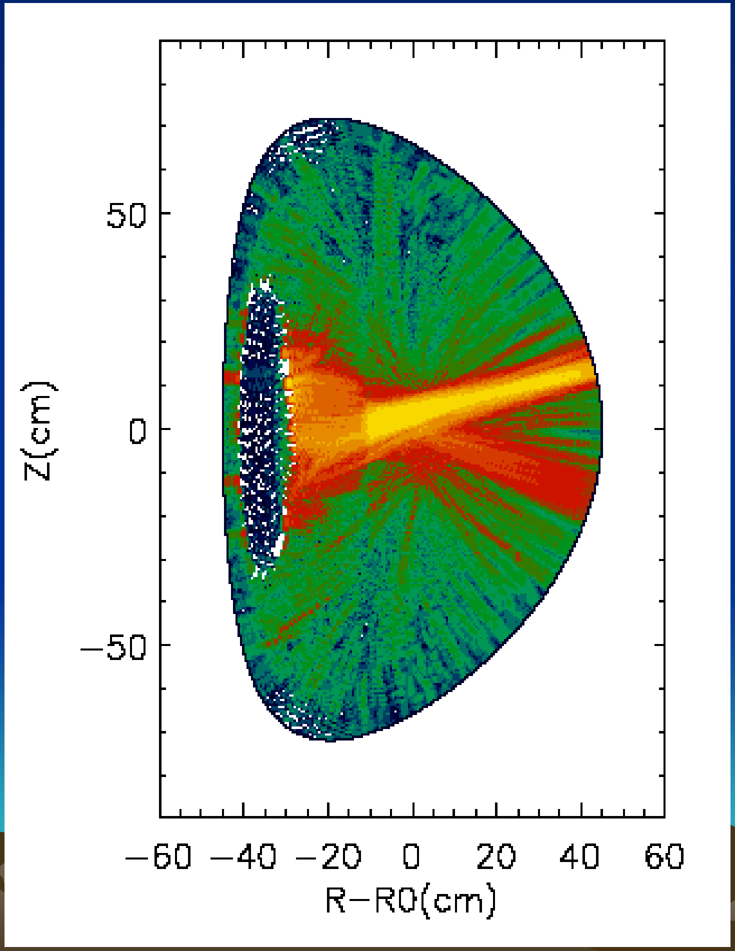

|Re(E_parallel)| **O-mode – no cut off**

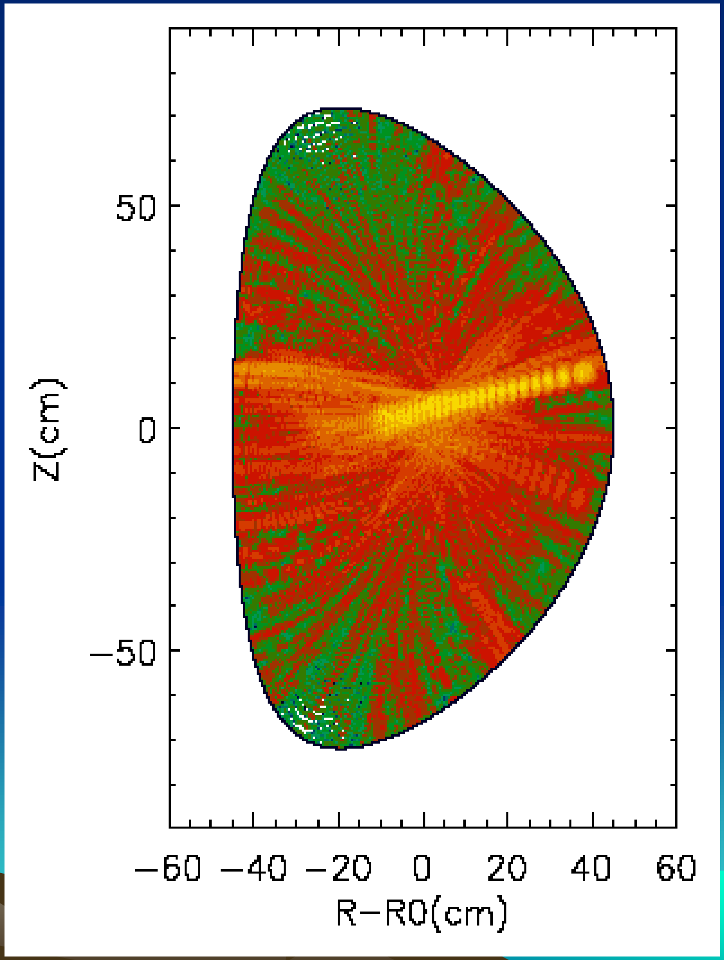

AUG ECH |(E_minus)| second harmonic X-mode outside equatorial launch to H-mode plasma

F=140 GHz, B_o=2.5T, I_p=0.72 MA, $N_{//}(0)$=0.076,

$N_e=1.0\text{x}\,10^{20}\ m^{-3}$, Te(0)=5.6 keV, α_n=0.15 $N_{cut\ off}$usual=1.25 $10^{20}\ m^{-3}$

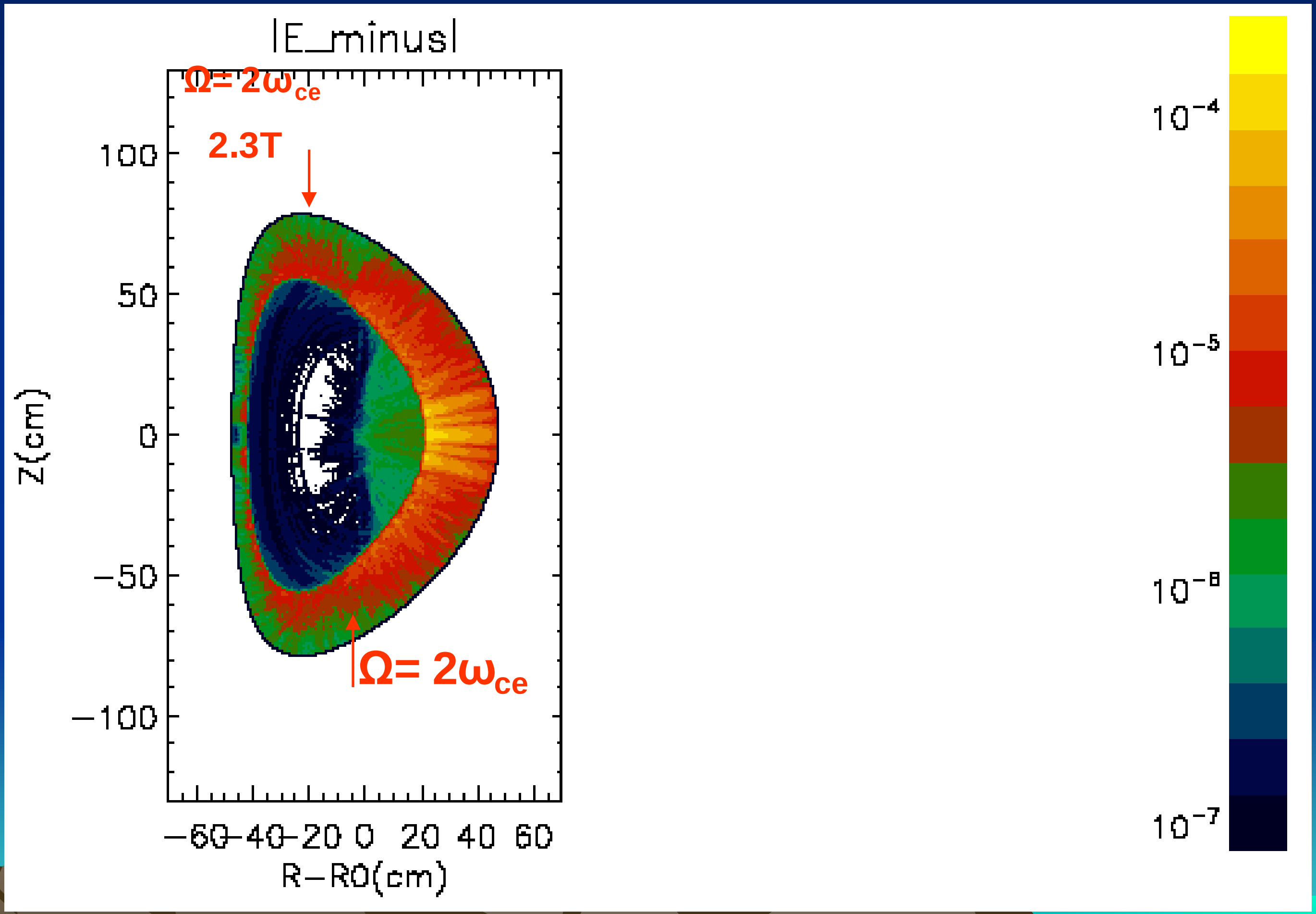

STELEC full wave ECH code:
Peripherical ECH power deposition in H-mode AUG dense plasma at 140 GHz – changes W ionization states chain

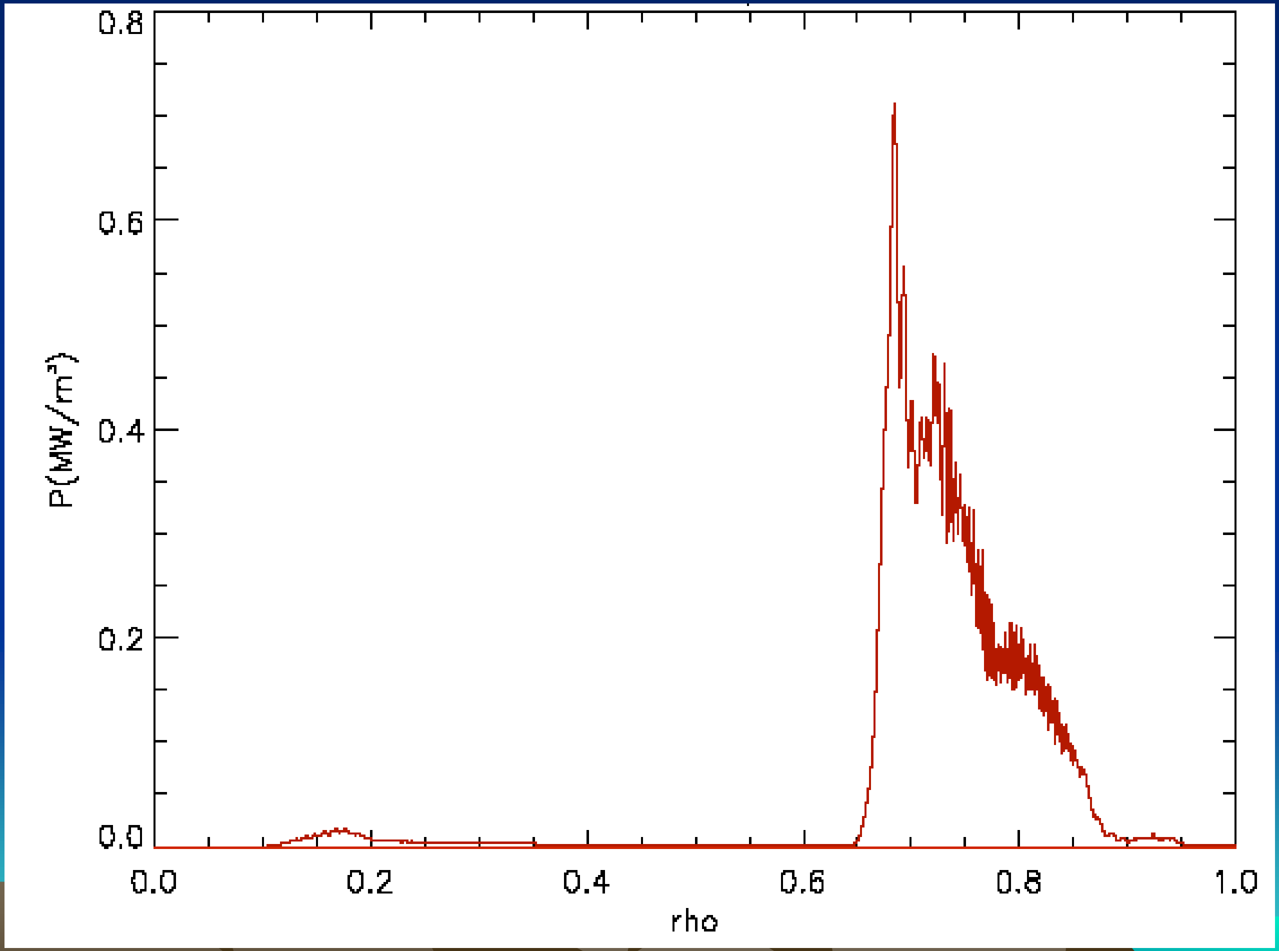

Second harmonic X-mode density cut off in tokamaks Importance of accounting to poloidal modes - N_Y They decrease density cut off level - analytical treatment, supporting STELEC findings

$$X = \frac{\omega_{pe}^2}{\omega^2} = \left(1 - \frac{\omega_{ce}}{\omega}\right)\left(1 - \frac{1}{2}n_y^2\right)$$

$$X = \frac{\omega_{pe}^2}{\omega^2} = 1 - \frac{1}{2}n_y^2 - \frac{\omega}{\omega_{ce}}\sqrt{1 - n_y^2}$$

Conclusions on X-mode density cut offs

- Exact Maxwell-Vlasov equations boundary value problem solutions for ECH for AUG and JET plasma by STELEC code clearly demonstrates decreased density cut off's with related power deposition at plasma periphery
  - modified interpretation of W wall AUG experiments
- STELEC code runs in non relativistic version show that decreased density cut offs still persist

O-X-B scenario for over dense plasma at second harmonic at 82.7 GHz in TCV

$N_e(0)=7\ 10^{19}\ m^{-3}$, $T_{eo}=1.97$ kV, $B_o=1.45$ T, Ip=415 kA, $N_{//}=0.277$

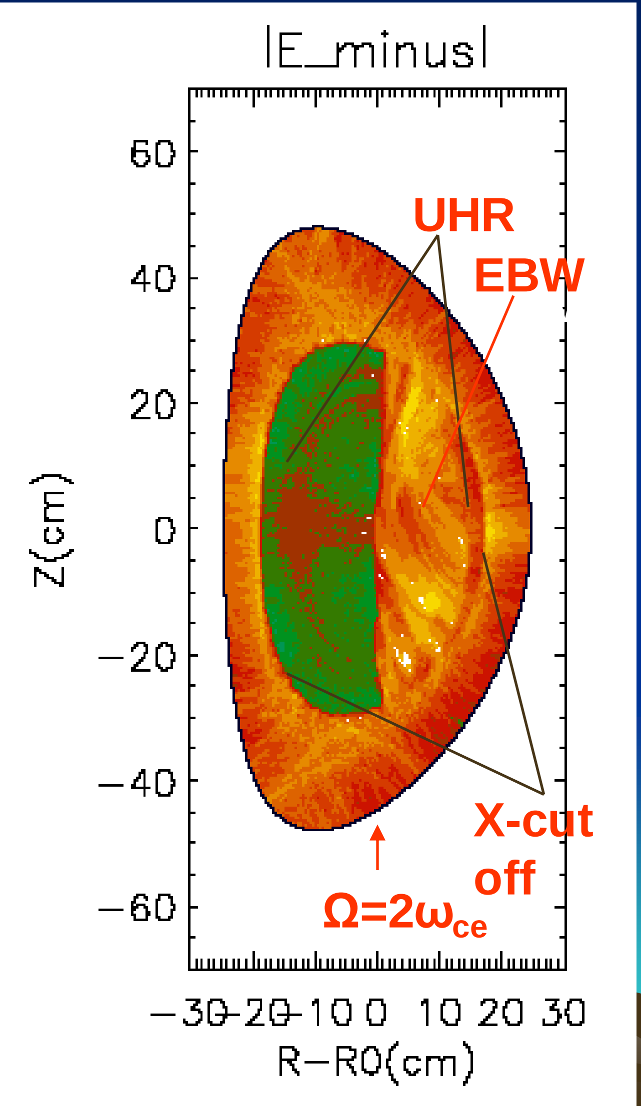

TCV ECH second harmonic O-mode outside equatorial

$N(0) = 7\ 10^{19}\ m^{-3}$ $T(0) = 1.97$ keV launch, F=82.7 GHz, $N_{//}(0)=0.277$

Power deposition from coupled X and O-modes

For X-mode the TCV plasma is over dense one

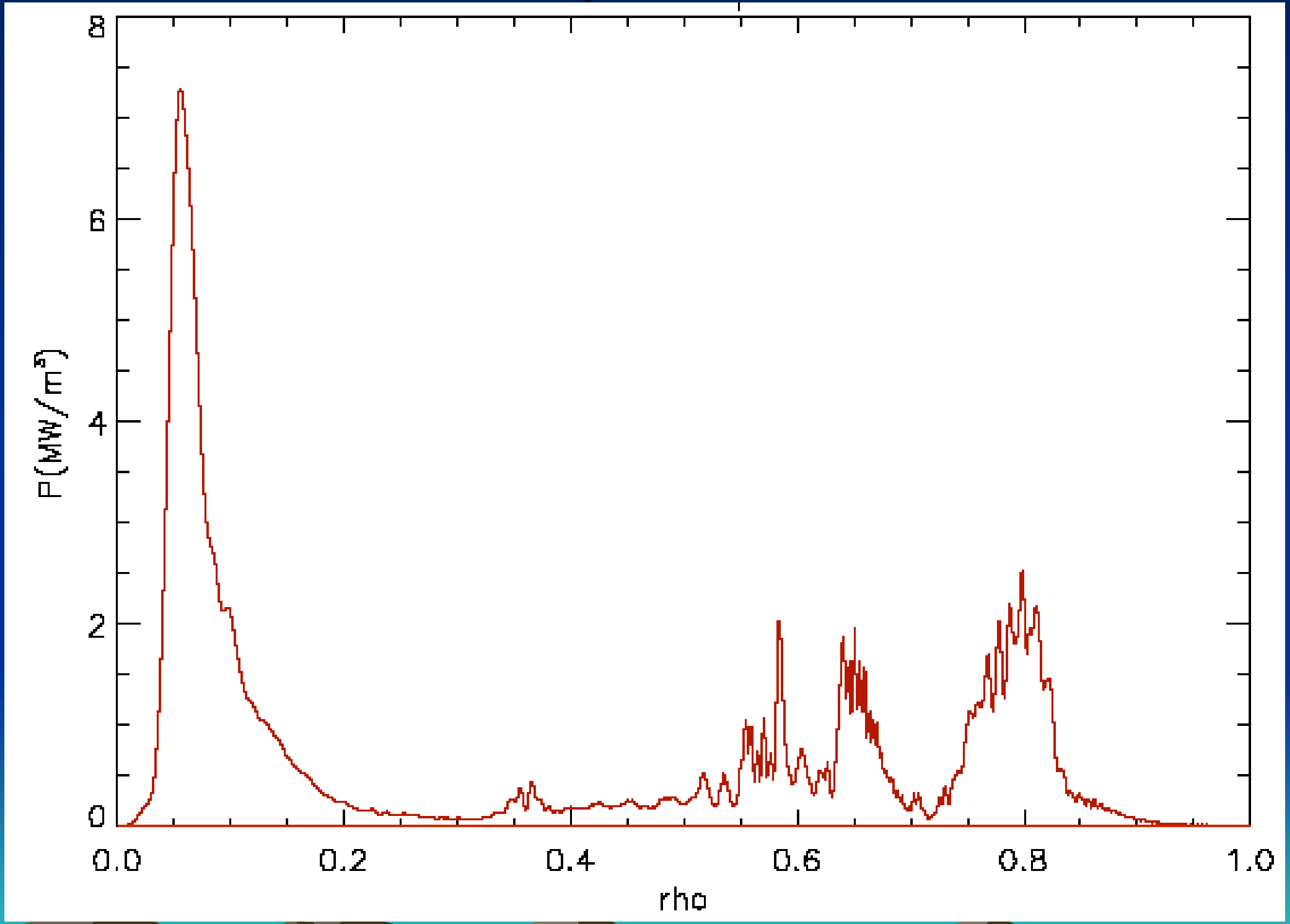

Similarity laws at ECH frequency range

Analysis of plasma RF induced currents, including FLR corrections, shows only appearance the parameters combinations:

$$\frac{\omega_{pe}^2}{\omega^2}, \quad \frac{\omega_{ce}}{\omega}, \quad T_e, \quad N_{//}$$

$$a >> \frac{1}{2\pi N_\perp}\lambda_0$$

ECH similarity laws check for non active ITER at B_o=2.65 T

X-mode second harmonic for F=30.3, 20 .2 and 10.1 GHz

NTM scenario upper port launch with gaussian beam divergence $\pm$0.71° and $N_{//}$ = 0.09 (STELEC code)

F=30 .3 GHz

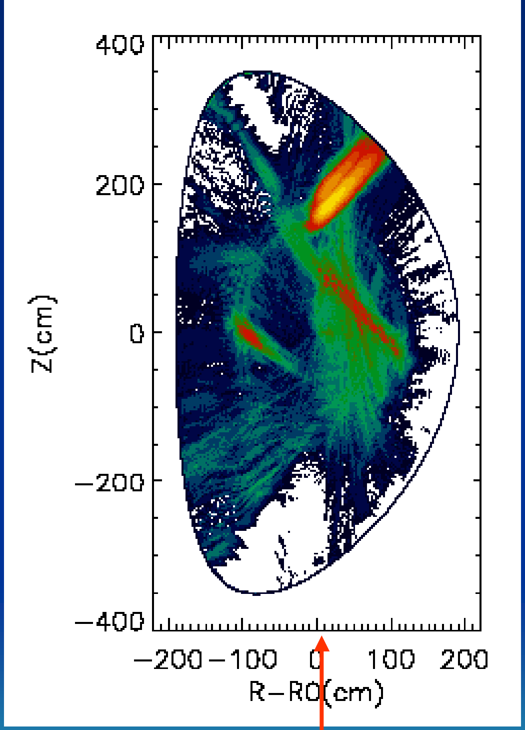

$\Omega = 2\omega_{ce}$

|ReE_psi| **F=20 .2** GHz

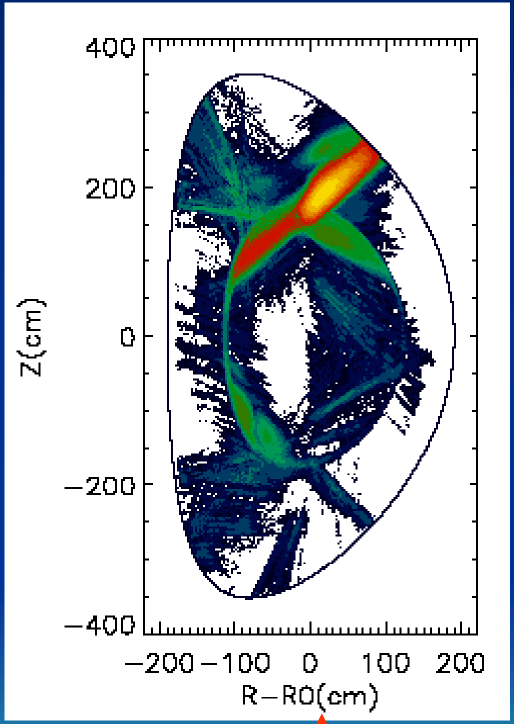

$\Omega = 2\omega_{ce}$

F=10 .1 GHz

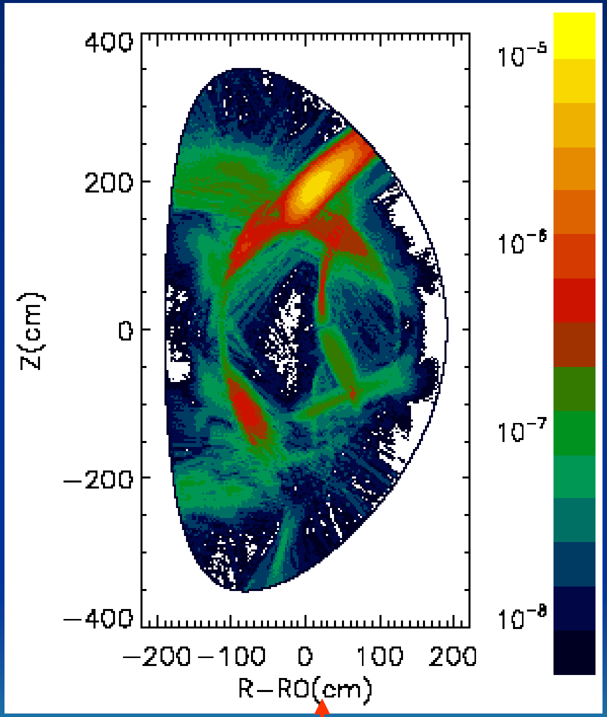

$\Omega = 2\omega_{ce}$

ECH power deposition in non active ITER at X-mode second harmonic for F= 30.3, 20 .2 and 10.1 GHz

F=30 .3 GHz

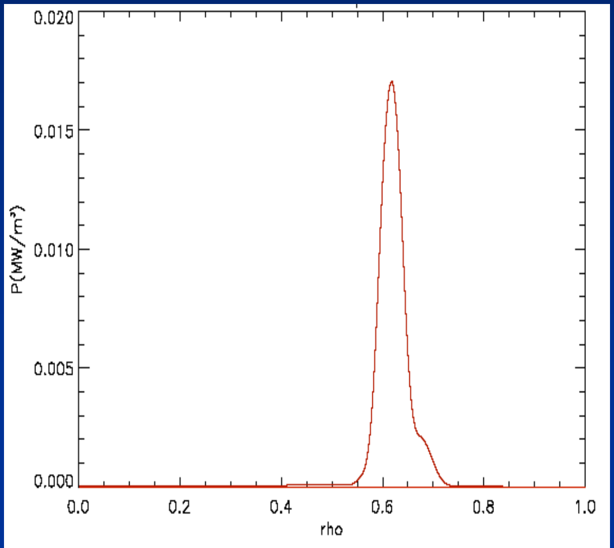

F=20 .2 GHz

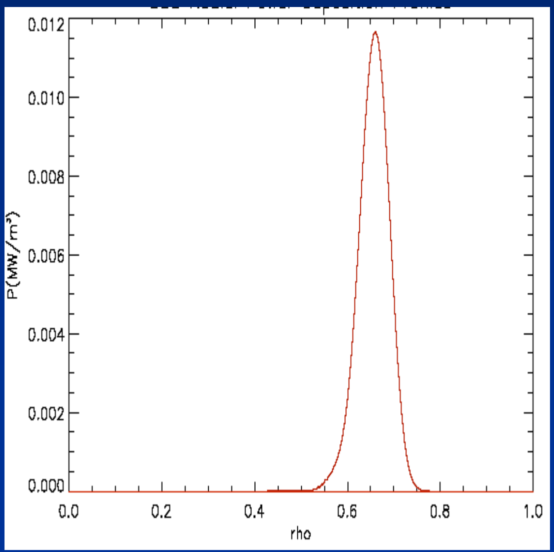

F=10 .1 GHz

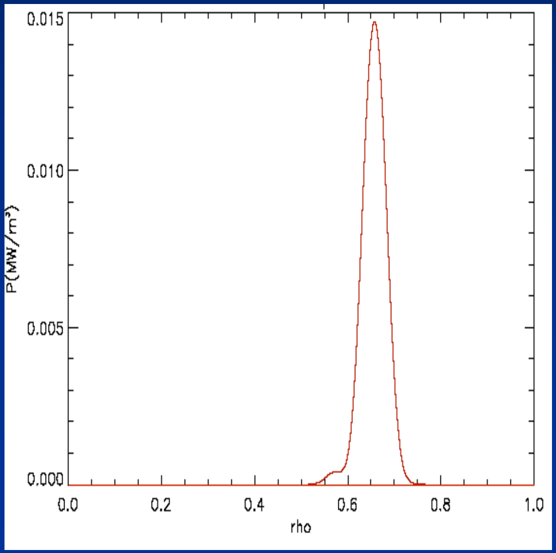

Conclusions

- Updated ECH STELEC code fundamental and second harmonic O- and X-mode STELEC modelling for middle tokamaks, JET and ITER plasmas shows
- - O-mode is coupled with X-mode
    probably through plasma toroidicity and wave reflection from plasma with following depolarization at the wall
  - O-mode at fundamental reveals broadened power deposition due to UHR appearance with mode conversion to EBW
    At oblique launch UHR space position governs power deposition
  - O-mode at second harmonic has some advantages in AUG, JET and ITER in dense plasma regimes
  - Observed X and O-modes coupling may lead
    to TWO power depositions at 2d harmonic in different plasma regions
  - Choice of ~170 GHz gyrotron in JET and ITER at half magnetic field and antennae with O and X-mode operation capability at second harmonic provides broader operation space

CONCLUSIONS (ctd)

- Second harmonic X mode scenarios in T-10, DIII-D JET, AUG, TCV and ITER evidently show more broader power deposition profiles in compare with usual ray tracing ones at moderate plasma densities. At low densities ray tracing still works
- Refraction and diffraction effects in rare and dense plasmas were modelled for T-10, DIII-D, TCV tokamaks in circular and elongated magnetic configurations
- Recent STELEC code modelling for non active ITER phase plasma in frequency range 5 – 30 GHz confirmed validity for similarity laws use at reduced frequencies for large fusion machines
- Decreased X-mode density cut offs (~20%) were discovered at second harmonic